DOI: 10.1002/smll.202000146

Intracellular labeling with extrinsic probes: delivery strategies and applications

*Jing Liu, Juan C. Fraire, Stefaan C. De Smedt, Ranhua Xiong, Kevin Braeckmans**

Dr. J. Liu, Dr. J. C. Fraire, Prof. Dr. S. C. De Smedt, Dr. R. Xiong and Prof. Dr. K. Braeckmans

Laboratory of General Biochemistry and Physical Pharmacy, Faculty of Pharmacy, Ghent University, Ghent B-9000, Belgium

Prof. Dr. S. C. De Smedt and Prof. Dr. K. Braeckmans

Centre for Advanced Light Microscopy, Ghent University, Ghent B-9000, Belgium

* Corresponding author: kevin.braeckmans@ugent.be

Keywords: intracellular labeling, extrinsic probes, microscopy, biomedical agents, cell-membrane disruption

Abstract

Extrinsic probes have outstanding properties for intracellular labeling to visualize dynamic processes in/of living cells, both *in vitro* and *in vivo*. Since extrinsic probes are in many cases cell-impermeable, different biochemical and physical approaches have been used to break the cell membrane barrier for direct delivery into the cytoplasm. In this review we will discuss these intracellular delivery strategies, briefly explaining their mechanisms and how they have been used for live-cell labeling applications. Methods that will be discussed include two biochemical agents that have been used for this purpose, which are cell penetrating peptides (CPPs) and the pore-forming bacterial toxin streptolysin O (SLO). Most successful intracellular label delivery methods are, however, based on physical principles to permeabilize the membrane and include electroporation, laser-induced photoporation, micro-/nanoinjection, nanoneedles or nanostraws, microfluidics and nanomachines. The strength and weakness of each strategy are discussed with a systematic comparison provided in the end. Finally, we summarize all the extrinsic probes that have been reported for intracellular labeling so-far, together with the delivery strategies that were used and their performance. This combined

information should provide for a useful guide for the reader to choose the most suitable delivery method for the desired probes.

1. Introduction

Cells are the basic building blocks of living organisms with sophisticated molecular processes happening both between and within them. As these processes involve the spatiotemporal dynamics of various biomolecules, including proteins, lipids, metabolites, nucleic acids and more, it is of great value to be able to observe them within the native cellular context for a deeper understanding of cell biology and diseases that are connected to these processes. Time-resolved optical and fluorescence microscopy are at present still the most optimal technique to observe such processes within living cells. Due to the crowded intracellular environment, the relevant molecules and organelles need to be labeled in order to study them selectively. While genetically encoded fluorescent proteins (FPs) have proven invaluable for this, the use of extrinsic probes remains of great interest as they can be more easily engineered for a broad spectral range, high brightness and photostability. Examples are illustrated in Figure 1 ordered according to their sizes, such as organic dyes[1], inorganic nanoparticles like quantum dots (QDs)[2] and carbon dots[3], and fluorescent polymeric nanoparticles.[4]

Apart from microscopy, labels are of importance for high-contrast *in vivo* cell tracking as well, which is of relevance not only to study natural cell migration processes, but also for the development of cell-based therapies where it is of interest to follow the fate of transplanted therapeutic cells to better understand the treatment outcome.[5-7] While fluorescent probes can be used for imaging in small animals, magnetic resonance imaging (MRI) contrast agents are of greater interest for larger animals and humans.[8] Common MRI contrast agents are Gd^{3+}-complexes and superparamagnetic iron oxides nanoparticles (SPIONs).[9, 10]

Regardless of the imaging technology, live-cell imaging applications generally require probes to be delivered inside cells. As cell probes come in a wide range of types and sizes, as some exemplary intracellular probes shown in Figure 1, getting them across the plasma membrane is,

however, a great challenge. Borrowing from the gene therapy field, cell-impermeable contrast agents can be internalized to some extent by endocytosis in a compound/cell-type dependent manner. For instance, the intracellular delivery by means of non-viral nanoparticles has been tried as well to stimulate the uptake of probes such as QDs[11] and labeled antibodies.[12] Generally, this is of little avail since endocytosed materials are mostly routed towards endolysosomes, meaning that the label-containing nanoparticles will be entrapped in endosomal vesicles for degradation.[13] Combined with low efficiency of endosomal escape for the currently available carrier systems[13-15], it means that probes are in any case not able to reach their target structures which generally are outside of the endosomes.

Therefore, to improve the endosome escape or bypass the endocytosis process, different biochemical and physical approaches have been used to enable extrinsic probes to get across the cell membrane and directly enter the cytoplasm. Biochemical approaches include the use of nanocarriers, CPPs and pore forming bacterial toxins, while physical methods include electroporation, laser-induced photoporation, micro- and nanoinjection, micro- and nanostructure mediated membrane disruption and the upcoming use of nanomachines or nanomotors. In this review, we will give a systematic overview of these methods and how they were used for delivering probes into live cells. For each strategy, the delivery mechanism will be briefly discussed as well as its performance for intracellular label delivery with a critical discussion on the advantages and disadvantages. Reported applications of the delivery methods will be summarized as well. Finally, we will give a discussion on potential future developments in this area.

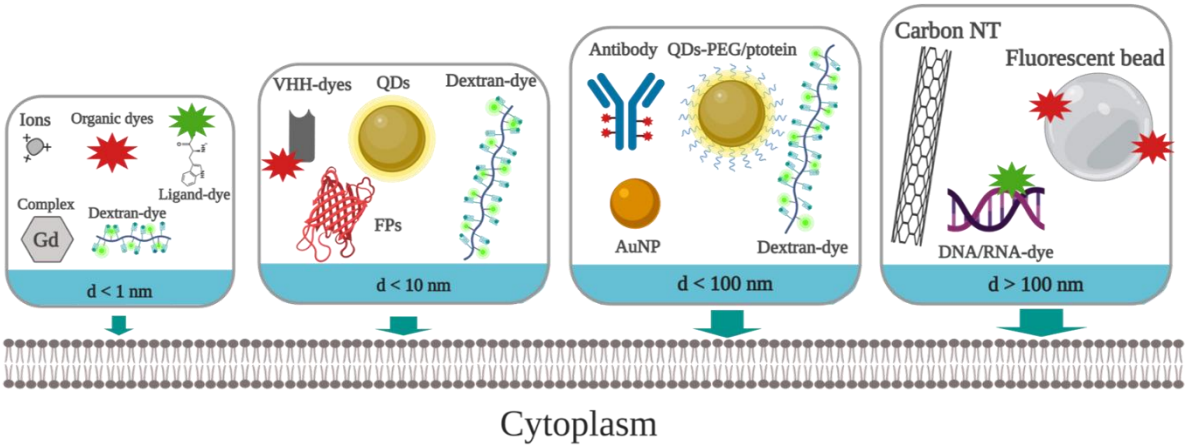

Figure 1. Extrinsic probes for intracellular labeling of live cells come in a wide variety of types and sizes. Different types of probes are ordered from small to large. The smallest ones have a size < 1 nm and include ions, organic dyes, organic dye conjugated ligands, inorganic complexes and organic dye-labeled dextran. Probes between 1 and 10 nm include fluorescent dye-labeled VHH (nanobodies), quantum dots (QDs), organic dye-labeled dextrans, fluorescent proteins (FPs). Probes between 10 and 100 nm include fluorescent dye-labeled antibodies, functionalized QDs, gold nanoparticles (AuNP), organic dye-labeled dextran. The largest probes exceed even 100 nm and include carbon nanotubes (NTs), fluorescent dye-labeled beads, and fluorescent dye-labeled RNA or DNA. Created with BioRender.

2. Biochemical strategies for delivering extrinsic probes into the cytoplasm

Borrowed from the drug delivery field, a first way to achieve intracellular translocation of labels is by using nanocarriers, such as lipid-based nanoparticles, polymeric nanoparticles, ligands conjugates, inorganic nanoparticles and virus like particles (VLPs) (Figure 2).[16] Most of these nanocarriers enter cells by endocytosis, meaning that most of them will be entrapped inside endosomes. To bypass endocytosis and deliver labels directly into the cytosol, biochemical agents can be used that increase the permeability of cell membranes. The best-known examples are cell penetrating peptides (CPPs) and the pore-forming bacterial toxin streptolysin O (SLO). Below we give an introduction into these various biochemical delivery strategies and how they have been used for intracellular label delivery.

2.1 Nanocarriers

Nanocarrier systems are widely used for gene and drug delivery due to a number of attractive features, such as their small size, tailorable ligands and ability to be loaded with various types

of cargo molecules. It comes as no surprise that they have been tried for the intracellular delivery of cell-impermeable labels as well. Lipid-based nanocarriers are among the most common drug delivery nanoparticles, being made from natural or synthesized lipids such as fatty acids and phospholipids.[17] They have been used to encapsulate probes, such as quantum dots (QDs). Al-Jamal *et al.* functionalized QDs with liposome to form cationic hybrid nanoparticles for living-cell labeling.[18] High efficient labeling of tumor cells was achieved this way in an ex vivo model, thus holding promise for long-term in vivo imaging of labeled cells in the future. Feng et al. used fusogenic cationic lipids to coat fluorescent polymer nanoparticles, demonstrating by fluorescence microscopy that they could be successfully delivered to the cytoplasm of cells.[19]

As mentioned above, inorganic nanomaterials have been used as intracellular labels, such as carbon-based materials and QDs.[20, 21] However, due to the endocytosis, it is difficult for those labels to enter the cytosol for specific targeting. To overcome the endosomal barrier, different ligands are conjugated to the surface to increase the endosomal escape, such as by cationic polymer coating, which is comprehensively reviewed by Qin et al..[17] Fluorescent QD is a good example for intracellular labeling by surface modification. Medintz et al. have reported different surface-capping and bioconjugation strategies of QDs for intracellular delivery, therefore achieving specific cellular labeling.[22] Besides labels, inorganic nanomaterials, such as mesoporous silica nanoparticles and carbon-based nanomaterials are also used as nanocarriers due to the large loading capacity and easy-to-modify surface for intracellular delivery of labels.[23] As a two-dimension material, graphene-based material has large and easy-to-adjust surface, making it an ideal nanocarrier for intracellular delivery.[24] Zhou et al. loaded the graphene oxide (GO) with Fe_3O_4 to get the GO/Fe_3O_4 hybrids for intracellular labeling, showing efficient cellular magnetic resonance imaging.[25] Zhang et al. facially incorporated aggregation-induced emission (AIE) materials into mesoporous silica

nanoparticles for cancel cell imaging, demonstrating excellent biocompatibility and strong fluorescence of the labeling.[26]

Polymeric nanocarriers have been used for intracellular delivery of labels as well. For instance Bayles et al. synthesized cationic core-shell acetalated dextran polymer colloids for delivery of nanocrystals, like QDs, and used them for monitoring protein-protein interactions in live cells by single particle tracking.[27] Nanogel nanoparticles, composed of cross-linked dextran polymer networks, are widely used in the intracellular delivery field, such as drug and gene.[28, 29] Owing to the ability of conjugation with multiple moieties, nanogels are used for intracellular delivery of different extrinsic labels. Toita et al. reported the intracellular delivery of protein-conjugated QDs by cationic $CHPNH_2$ nanogel into mesenchymal stem cells, showing a long-term tracing by fluorescence microscopy.[30] Chiang et al. used the hollow hybrid nanogels to load the citric acid-coated superparamagnetic iron oxide nanoparticles as well as drug for intracellular delivery, demonstrating the guidable delivery of stimuli-mediated diagnostic imaging and hyperthermia/chemotherapies.[31]

Inspired by the vaccines for human papilloma and hepatitis B viruses, VLP have been mostly used for intracellular delivery of genes and proteins.[16] They have been explored for probe delivery as well by attaching labels on the surface or loading them inside the VLP. For instance, this way Savithri and coworkers have used VLPs with antibodies attached to the surface for intracellular deliver into live cells for tubulin labeling.[32] Gag-GFP fusion protein could also be incorporated into the cytosol by loaded in VLP, with an efficiency of almost 100%.[33]

Biochemical nanocarriers are attractive to consider for probe delivery as many can be readily borrowed from the drug delivery field. In many cases biomedical nanocarriers are relatively cheap and easy to use. However, often specific chemical modifications are necessary to load them with probes, which are physiochemically different than, let’s say, nucleic acids. Most

nanocarriers enter cells by endocytosis so that they reside inside endosomes, most of which are eventually trafficked to acidic degradative endolysosomes.[34] While this may lead to quenching and label degradation, this may not be an inherent problem if the aim is to label whole cells for (in vivo) cell tracking.[14, 35] However, for microscopy this is more problematic since here the purpose is to label specific subcellular structures. For that, the labels need to be release from the carriers and endosomes, which is one of the most important bottlenecks on the intracellular level for nanocarriers.[14, 36] As a consequence, even if a fraction of the labels is released from the endosomes, it still results in a confounding staining of labeled endosomes and the targeted structure. Therefore, other strategies that allow direct access to the cytosol are generally preferred for label delivery for microscopy.

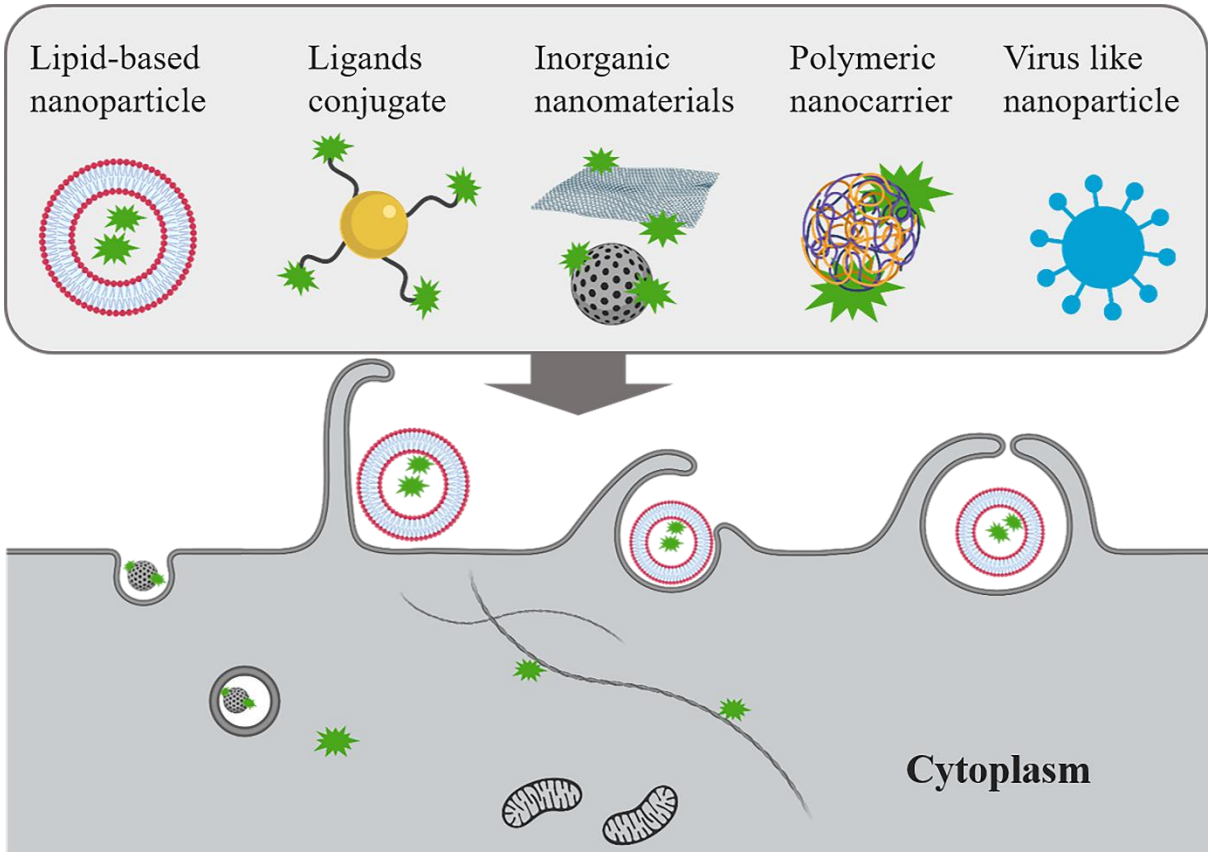

Figure 2. Different types of nanocarriers used for intracellular delivery of labels through different endocytosis processes. The listed nanocarriers are lipid-based nanoparticle, ligands conjugates, inorganic nanomaterials, polymeric nanocarrier and virus like particles. The scheme

illustration below shows different endocytosis processes, which are pinocytosis (first left one) and phagocytosis (right three). Created with BioRender.

2.2 Cell penetrating peptides

Since the trans-Activator of Transcription (Tat) protein has been demonstrated to be able to efficiently enter into cultured cells in the 80s, the family of CPPs rapidly expanded to other peptides as well.[37, 38] In general, CPPs are short peptides, mostly with positively charged sequences of amino acids, with the capacity to cross cellular membranes. Based on their origin, one discriminates three classes of CPPs, including peptides derived from proteins, chimeric proteins and synthetic peptides.[39, 40] A detailed account of the classification of CPPs with their properties has been reviewed elsewhere.[41] By conjugating CPPs to the compound of interest, they have been used for the intracellular delivery of various types of compounds, such as nanoparticles (NPs), other peptides, proteins, nucleic acids (oligonucleotides, cDNA, RNA, siRNA), contrast agents for magnetic resonance imaging, and therapeutic compounds.[42, 43]

The manner in which CPPs find their way into cells is still a matter of debate. In general terms there are two mechanisms involved, being on the one hand direct translocation across the plasma membrane into the cytoplasm, and on the other hand endocytic uptake (Figure 3a). The involvement of each mechanism is influenced by the physicochemical properties of the peptides, characteristics of the cargo molecules to which they are conjugated, cell conditions, temperature, PH, and so on.[44, 45] For the direct translocation of the CPPs, several hypotheses were reported to explain the underlying mechanism based on a strong electrostatic interaction of the cationic CPPs with the negatively charged phospholipids in the cell membrane.[39] The first hypothesis is the formation of inverted micelles causing the translocation of CPPs towards the cytoplasm (Figure 3b). The second hypothesis is the formation of transient toroidal pores with a size up to 2.5 nm through which the CPPs can migrate (Figure 3c).[46, 47] The third hypothesis is the carpet model which suggests a direct translocation of the CPPs through the

phospholipid bilayer driven by the membrane potential (Figure 3d).[44] Still, other mechanisms have been proposed as well, for instance, the membrane-thinning model and electroporation-like permeabilization.[44, 48, 49] The disturbance of the cell membrane by those transient pores activates the membrane repair response because of the influx of extracellular calcium to reseal the injured cell membrane.[50]

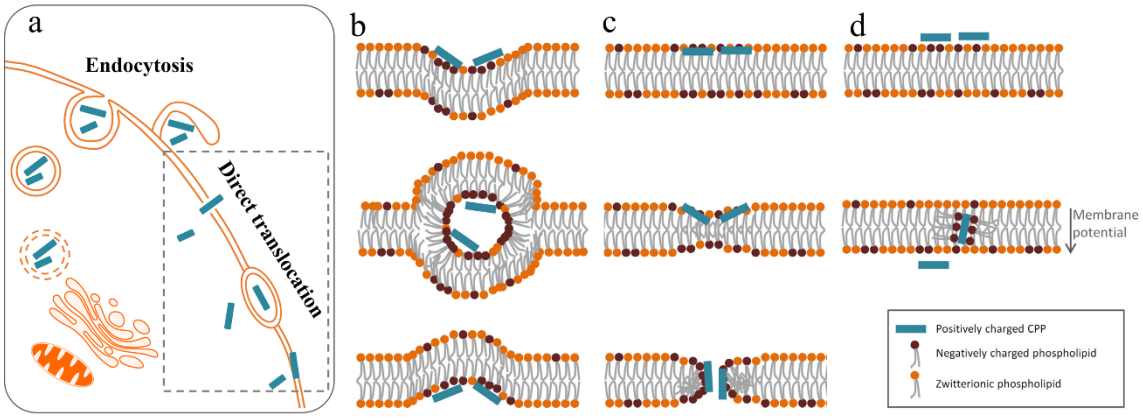

Figure 3. Intracellular pathways of CPPs passing through the cell membrane. **a.** The two major mechanisms of CPP entry into cells are endocytosis and direct translocation. **b-d** Schematic representation of the three main mechanisms of direct translocation, including **b.** inverted micelle formation, **c.** pore formation, **d.** carpet model. Figure modified from Koren *et al.* and Bechara *et al.*[39, 40] and reproduced with permissions from Elsevier and John Wiley and Sons.

CPPs, conjugated to probes, have been used to label cells. For instance, fluorescein-labeled Tat-peptide was shown to successfully stain the cytosol as well as the nucleus of Jurkat and KB 3-1 tumor cells (Figure 4a).[51] In another report, amphiphilic CPPs could transport three types of thermally activated delayed fluorescence (TADF) molecules into living cells for time-gated imaging (Figure 4b).[52] Recently Ji *et al.* labeled the paclitaxel (PTX)-locked nucleic acid (LNA)-Tat nanomicelle with FITC for both cell fluorescence imaging and drug delivery (Figure 4c).[53] Also Tat peptide-conjugated quantum dots (Tat-QDs) could be actively transported into cells and was used as a model system to examine the cellular uptake and intracellular transport of nanoparticles in living cells (Figure 4d).[54] Lei *et al.* used Tat-QDs to efficiently label mesenchymal stem cells for *in vivo* cell tracking.[55] Recently Yong *et al.* reported to greatly enhance the delivery of such Tat-QDs into the cell's nucleus by adding a small

percentage (e.g. 1%) of organic solvent.[56] For specific labeling and imaging of subcellular structures, camelid-derived single-chain VHH antibody fragments, also termed nanobodies (Nb), were conjugated with arginine-rich cyclic CPPs (cR10).[57] These GFP-targeting CPP-nanobodies were taken up by ~ 95 % cells by a non-endocytic process within one-hour incubation, consequently relocalizing the GFP into the nucleolus by the GFP-binding nanobody with conjugated arginine-rich CPP which has an affinity for RNA within the nucleolus. Since the arginine-rich CPPs have a high affinity for RNA, they were found to associate strongly with the nucleolus (Figure 4e). Finally, Dendrimeric nanoparticles coated with activatable cell-penetrating peptides (ACPPs), labeled with Cy5, gadolinium, or both, have been shown to be useful for dual fluorescence and MRI imaging of tumors (Figure 3f).[58]

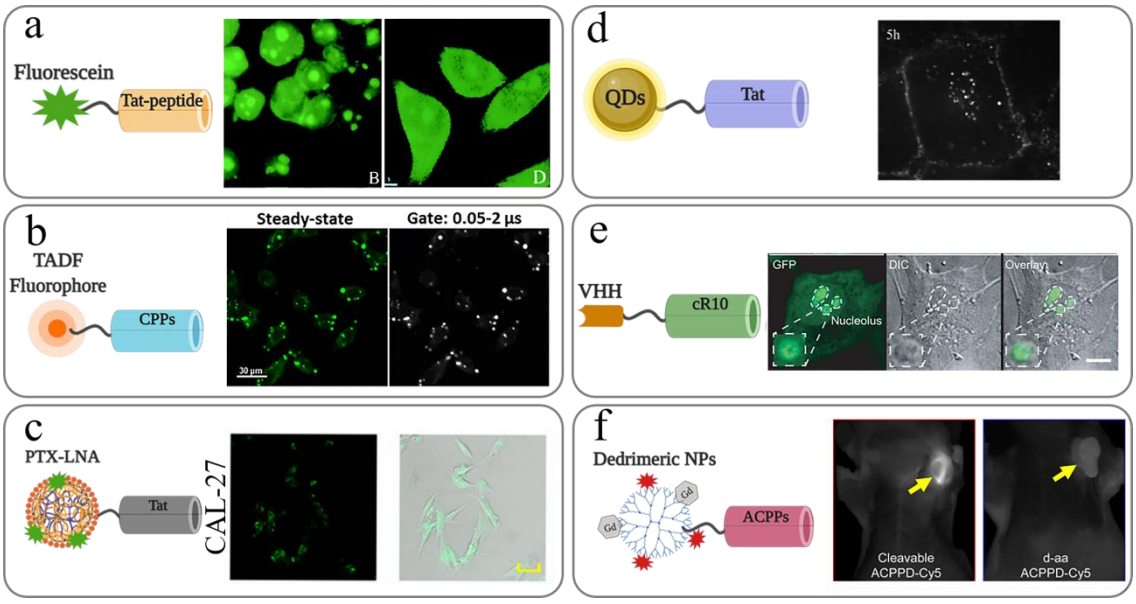

Figure 4. Intracellular labeling with extrinsic probes conjugated to CPPs. **a.** Cellular accumulation of a fluorescein-labeled Tat−peptide conjugate. Confocal images of human Jurkat cells after incubation with Tat−peptide at 37 °C (left) and KB-3-1 tumor cells after incubation with Tat−peptide at 37 °C (right). Reproduced from Polyakov *et al.*.[51] and produced with permission from American Chemical Society. **b.** Time resolved luminescent imaging of cells labeled with TADF-CPPs. Illustration of TADF fluorophore-labeled Tat-peptide (left), steady-state (middle) and time-gated (right) fluorescence images of HeLa cells after incubation with CPP-functionalized 4CzIPN (one TADF fluorophore). Reproduced from Zhu *et al.*.[52] and produced with permission from American Chemical Society. **c.** Illustration of PTX-LNA-Tat nanomicelle labeled with FITC (left). Confocal laser scanning microscopy images of CAL-27 cells after incubation with PTX-LNA-TAT. Scale bar is 10 µm. Reproduced from Ji *et al.*.[53] and produced with permission from American Chemical Society. **d.** Illustration of QDs conjugated with Tat (left) and time-dependent imaging of Tat-QD uptake and intracellular

transport in cultured HeLa cells after 5 h (right). Reproduced from Ruan *et al.*.[54] and produced with permission from American Chemical Society. **e.** Illustration of an anti-GFP nanobody (VHH) conjugated with arginine-rich cyclic CPPs (cR10) (left). Confocal images of 3T3 cells expressing GFP and incubated with 20 μM of VHH–cR10 for 1 h. Reproduced from Herce *et al.*.[57] and produced with permission from Springer Nature. **f.** Illustration of dendrimeric nanoparticles coated with ACPPs (left). Representative fluorescence images 48 h after injection with ACPP-Cy5 in tumors (middle and right). Reproduced from Olson *et al.*.[58] and produced with permission from PNAS. Created with BioRender.

Even though CPPs are regarded as a powerful tool to transport cell-impermeable labels into living cells, they come with some limitations as well. CPPs can induce cytotoxicity to cells due to their high cationic charge, especially at higher doses. For instance, leakage of the cell membrane has been reported, as well as poor cell viability and cellular proliferation.[59],[60] In any case it needs to be carefully tested for each new construct as it was demonstrated that the cytotoxicity of CPPs highly depends on peptide concentration, cargo molecule and coupling strategy.[61] When aimed at selective imaging of specific intracellular targets, a second limitation comes from the fact that endocytosis is a major uptake route of the CPP-label conjugates.[14] Since at least a part of the internalized CCP-label is expected to remain trapped in endosomes, it will lead to a confounding double staining pattern of endosomes on the one hand and the actual target on the other hand.[45] A third more practical limitation is that conjugates need to be specifically made and tested for each type of (targeted) label so that its use likely will remain limited to specific cases.

2.3 Pore forming bacterial toxin streptolysin O (SLO)

Pore forming toxins (PFTs) form a broad class of proteins from bacteria, plants, fungi, and animals that can form pores in the plasma membrane of mammalian cells. Due to practical and safety reasons, the proteins from bacteria have attracted the most attention so far.[62] One family of pore forming toxins are the cholesterol dependent cytolysins (CDCs), which includes streptolysin O (SLO).[63] CDCs can bind to cholesterol complexes in cell membranes resulting in the formation of large pores through which molecules can pass. The mechanisms of CDC

pore formation have been reviewed by Hotze *et al.*.[64] In brief, the soluble CDC monomers bind to cholesterol in the membrane by initial monomer-monomer dimerization.[45] The dimers will then form homo-oligomeric doughnut-shaped pore complexes on the membrane, which is the pre-pore complex.[65] The conformation of the pre-pore complex subsequently changes, followed by the SLO dimers inserting into the membrane to form pores.[66] SLO can induce fairly large pores in the cell membrane, allowing the delivery of compounds up to 150 kDa as demonstrated with fluorescent dextrans of various molecular weights.[67, 68]

From a practical point of view, the diluted SLO solution is typically first mixed with the probes and then incubated with the cells for ~ 10 min at 37 °C.[67, 69, 70] In some cases, the SLO solution was added to the cells first (~10 min at 37 °C) before adding and incubating the probes for another ~ 5 min on ice.[68] An important step after the SLO treatment is allowing the cells to reseal by incubating with Ca^{2+}-supplemented medium.[71] The pores generated by SLO have been shown to be reversible with recovery time from 30 min to 2 h. A comprehensive discussion on the membrane repair mechanisms is given by Andrews *et al.*.[72] One important repair process widely believed to be involved is patching by exocytic vesicles that are triggered by Ca^{2+} influx.[71, 73]

Different molecules and proteins have been successfully delivered into living cells after SLO treatment for intracellular imaging. I. Walev *et al.* delivered different sizes of fluorescein-labeled dextran and albumin into adherent and nonadherent cells.[67] A luminescent terbium complex, TMP-Lumi4, was also delivered into living cells by SLO for studying protein-protein interactions.[69] Recently, Teng *et al.* used SLO for the delivery of different sizes of fluorescent labels for dSTORM super-resolution imaging, from small organic molecules, over fluorescently labeled Nb, to ligand binding proteins and antibodies.[68, 74]

While these examples show that probes can be successfully delivered by SLO treatment into cells, it comes with some limitations as well. As the PFTs are produced by different organisms that target different cells for different purposes, even within one family their performance is very much cell-type dependent.[75] Therefore, for every cell type the optimal type of PFT, its concentration and incubation time need to be screened in terms of delivery efficiency and cytotoxicity. Another limitation is that the pore size is limited to the entry of molecules < 150 kDa,[68] so that larger probes, like functionalized QDs, cannot be easily delivered by this method.

3. Electroporation

Stemming from the 1980s,[76] electroporation is arguably the best known physical permeabilization technique for the intracellular delivery of a broad range of components, including dyes, nanoparticles, proteins and multiple forms of DNA and RNA.[77] Cells are usually brought into suspension and treated with intensive electric pulses to transiently permeabilize the cell membrane. This is referred to as 'bulk electroporation' and will be discussed first below. Recently, newer electroporation technologies have appeared that are more suitable to treat adherent cells as well. These types of 'adherent electroporation' will be discussed afterwards.

3.1 Bulk electroporation

In conventional electroporation, cells are suspended in a conducting buffer and treated in cuvette-style parallel plate setups. The cuvettes have two electrodes on either site that are connected to a high voltage pulse generator. When an electric pulse is applied, a near-homogeneous electric field is created across the cell suspension which induces pores in the cell membrane. Details on the electric pulses and the process of pore formation are comprehensively reviewed elsewhere.[78, 79] Conveniently, multiple commercial electroporation devices are

currently available, such as the Neon™ Transfection System (Thermal Fisher Scientific) and the 4D-Nucleofector™ System (Lonza).

Despite being one of the most popular physical cell transfection technologies to date, bulk electroporation has been seldom used for the intracellular delivery of labels. Derfus *et al.* used electroporation to deliver negatively charged QDs into living cells but found that they formed aggregates up to 0.5 μm in the cytoplasm.[2] In one other report, organic fluorophore-labeled DNA fragments and proteins were delivered into bacteria (*Escherichia coli*) by electroporation for investigating the structural integrity and functionality of these molecules at the single-molecule level.[80]

The fact that bulk electroporation hasn't been used that often for labeling applications is likely connected to two important limitations. First of all, it is commonly observed that electroporated cells suffer from high acute toxicity, often resulting in fairly low numbers of cells that survive the treatment.[81] Secondly, since most commercial bulk electroporation devices only work with cells in suspension, this is rather cumbersome for imaging applications where cells are often adherent. Newer forms of electroporation may, therefore, be more promising for labeling applications, as discussed next.

3.2 Adherent electroporation

More recently, by combining nanotechnology with novel materials, new electroporation platforms have been developed that are better suited for the treatment of adherent cells. A nanoelectroporation platform with alumina nanostraws was developed by X. Xie *el al* for the delivery of organic dyes and plasmids.[82] Fluorescent probes are delivered from an underlying microfluidic channel through the nanostraws into cells that are cultured on top of them (Figure 5a) and which become permeabilized at the tips of the nanostraws upon application of electric pulses. Highly efficient intracellular delivery is achieved by a combination of diffusion through

the nanostraws and active electrophoresis during electric pulsing. More recently, Huang *et al.* developed a similar electroporation platform but used separate electrodes for electroporation and for electrophoresis of gold nanorods which could be detected by surface-enhanced Raman scattering (SERS) (Figure 5b).[83] The cell membrane is porated by the electroporation electrodes, while the gold nanorods are actively transported by a DC potential through the hollow nanoelectrodes. Based on a similar principle, a multifunctional branched nanostraw (BNS)-electroporation platform was developed by He *et al.* to perform analysis of circulating tumor cells (CTC) (Figure 5c).[84] After CTC capture by antibodies on the nanostraws, small fluorescent molecules were delivered, showing safe, efficient, and spatially controlled labeling. Kang *et al.* built a 'nanofountain probe electroporation' (NFP-E) device to precisely deliver molecules into single cells (Figure 5d).[85] Here the cell membrane is permeablized by a localized electric field generated at the NFP cantilever tip. With this device fluorescently labeled dextran could be delivered into single cells with > 95 % efficiency and high viability (92 %). Very recently, Moon *et al.* also achieved excellent spatially and temporally controlled intracellular delivery with a graphene-based electroporation device (Figure 5e).[86] With a mono-layer coating of graphene and voltage pulses, the platform was shown to be suitable for the intracellular delivery of fluorescent probes for *in situ* super-resolution microscopy on the same device.

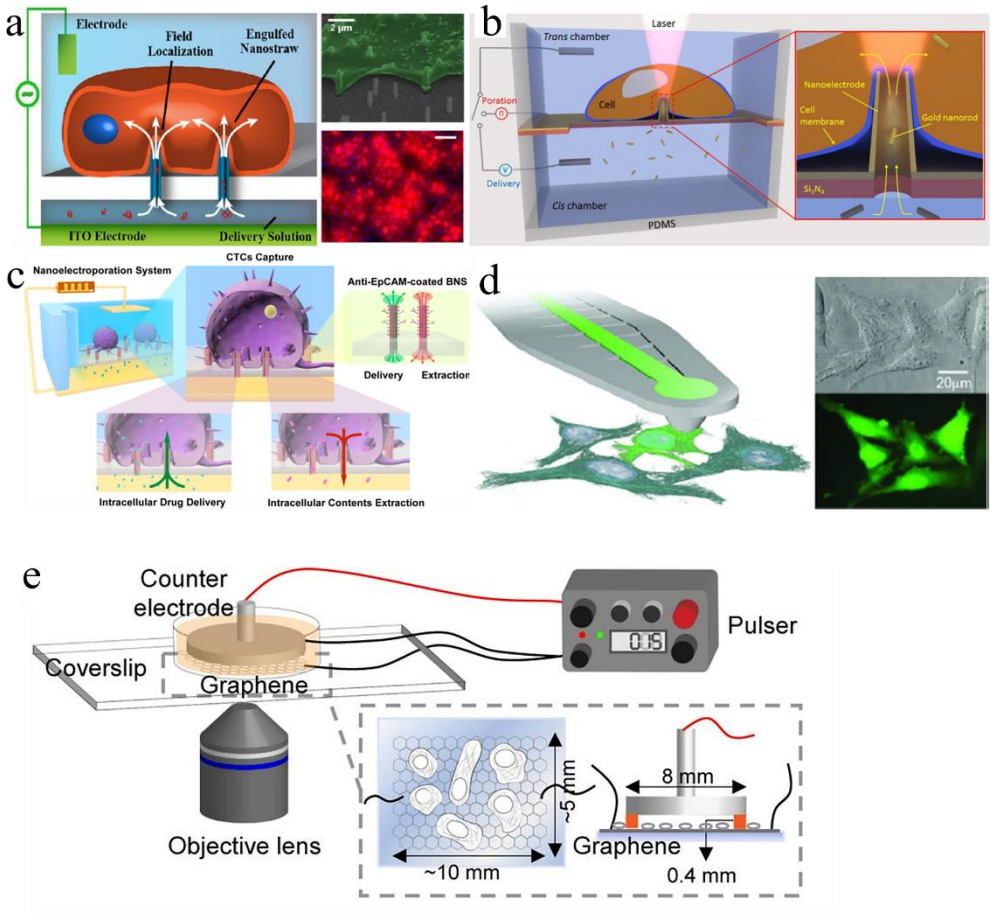

Figure 5. New generations of electroporation devices for delivery into adherent cells. **a.** A nanoelectroporation platform with alumina nanostraws for fluorescent dye delivery. Reproduced from Xie *et al.* and produced with permission from the American Chemical Society.[82] **b.** Schematic representation of the 3D hollow nanoelectrode device for single-particle intracellular delivery. The cell is tightly wrapped around the gold-coated hollow nanoelectrode and is first electroporated by applying voltage pulses. Then, the nanorods originally in the cis chamber are delivered into the cell through the hollow nanoelectrode by a DC potential between the two Pt wire electrodes. Inset: a laser beam excites the Raman signals of the delivered nanorods for counting the number of delivered nanorods. SEM images of 3D hollow nanoelectrode array on Si_3N_4. Reproduced from Huang *et al.* and produced with permission from the American Chemical Society.[83] **c.** Schematic illustration of the multifunctional BNS-electroporation system for capture of cancer cells, followed by in situ intracellular drug delivery and intracellular contents extraction. The BNSs were modified with specific biomolecules, anti-EpCAM, to specifically capture cancer cells, followed by integration with a microfluidic nanoelectroporation system for nondestructive cell poration. Reproduced from G. He *et al.* and produced with permission from American Chemical Society.[84] **d.** Schematic illustration of a NFP-E device (left) and representative microscopy images of cells labeled with dextran Alexa Fluor 488. Reproduced from W. Kang *et al.* and produced with permission from American Chemical Society.[85] **e.** Schematic of the experimental setup of electroporation of adherent cells on a graphene-covered glass coverslip. Reproduced from S. Moon *et al.*[86] and produced with permission from the authors.

While being more readily compatible with adherent cells, these novel electroporation platforms are still in the research phase and not yet readily available. Still, it shows that thanks to the

development of nanotechnology and material sciences, more precise and convenient electroporation platforms can be fabricated which holds great promise for the future. Since usually a lower voltage can be used, the adherent electroporation techniques come with better cell viability compared to bulk electroporation. On the other hand, adherent electroporation offers lower cell throughput than bulk electroporation and not all devices are readily compatible with microscopy after label delivery.

4. Laser-induced photoporation

Optical energy can be used as well to induce cell membrane permeabilization for the intracellular delivery of probes. We will discriminate three different approaches, the first being direct photoporation where individual pores are created in cell membranes with a tightly focused laser beam. In the second approach, the required laser intensity is reduced by using photosensitizing nanoparticles that efficiently absorb laser light and create pores in cell membranes by photothermal effects. In the third approach, cells are instead grown on photosensitive microfabricated substrates which can permeabilize the cell membrane upon laser irradiation through photothermal effects. These three approaches will be discussed sequentially below.

4.1 Direct laser-induced photoporation

In direct laser-induced photoporation a high-intensity pulsed laser beam is focused onto the cell membrane (Figure 6a) to create holes by a combination of thermal, mechanical, and chemical effects.[87] Direct photoporation, also termed optoporation, optoinjection or laserfection, was first reported in 1984 at which time an Nd:YAG UV laser with nanosecond (ns) pulses was used for plasmid DNA intracellular delivery.[88] In later years, a UV ns pulsed laser and a third harmonic (355 nm) of an yttrium-aluminum garnet laser were used as laser transfection technique for DNA delivery into different types of cells.[89, 90] In 2002, a breakthrough was

made by Tirlapur *et al.* in that they used an ultra-short 800-nm femtosecond (fs) pulsed laser for localized perforation of the cell membrane.[91] Plasmid DNA was delivered into cells through the membrane pores to achieve invariably 100% transfection efficiency and cell viability.

Direct photoporation was used for the delivery of different kinds of intracellular labels. A Nd:YAG pulsed laser with 532-nm output wavelength was used for the delivery of organic dyes and tetramethylrhodamine-dextran 3 kDa into different types of cells.[92] By controlling the laser scanning area, these compounds could be delivered in a spatially controlled manner. It was found that the cell membrane returned to its normal state in a very short time with limited cell damage at sublethal laser doses.[93] A Nd:YAG picosecond (ps) laser (1064 nm, pulse duration 17 ps) was used as well to perforate a single plant cell, demonstrating successful delivery of PI.[75] Once the fs laser became available, it was preferred over ns pulsed lasers as it could induce multiphoton effects to increase the perforation efficiency while reducing collateral damage to neighboring cells. Uchugonova *et al.* used a < 20 fs 792-nm pulsed laser to deliver ethidium bromide into living cells with very low laser power.[94] A similar approach (800 nm, pulse duration of 12 fs) was also used by Lei *et al.* in the same year to deliver propidium iodide (PI) into two different neuron cells. With NIR fs laser pulses (120 fs, 800 nm), direct photoporation was even successful in delivering fluorescent labels into living vertebrate embryos.[95] FITC labeled morpholinos (1810 Da) and dextran (10 kDa) were delivered into single cells in zebrafish embryos or chick embryos, showing 71% delivery efficiency. The cell impermeable label rhodamine phalloidin (1306 kDa), which stains actin filaments, was delivered into cells by fs (800-850 nm, 100 fs) laser-induced photoporation as well.[96] Nanomolar concentrations of rhodamine phalloidin was enough to label mammalian cells for further dynamic studies.

Although direct photoporation of the cell membrane with pulsed lasers enables efficient and non-toxic delivery of many types of molecules, the throughput is inherently low. Indeed, holes are created one by one by careful focusing of the beam precisely onto the cell membrane. To enhance throughput, a 'non-diffracting' Bessel beam has been proposed, which combines a small beam size with a near infinite depth of focus (Figure 6b). Combined with a microfluidic chip, the Bessel beam (800-nm, 140 fs) could achieve 26.6 % PI positive cells with a throughput of 10 cells·s^{-1}.[97] In any case, since fast and ultrashort fs lasers are very costly and require dedicated optical expertise, direct laser-induced photoporation has become replaced by newer approaches where the optical requirements are relaxed by the use of sensitizing nanoparticles or microfabricated substrates. These newer approaches offer similar benefits but at vastly higher throughput rates, as will be discussed next.

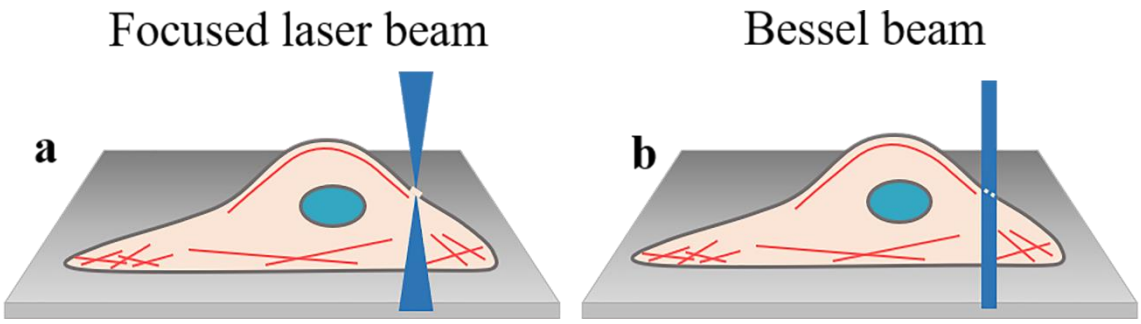

Figure 6. Direct laser-induced photoporation. **a.** Pores can be created in the cell membrane with a focused ns or fs pulsed laser beam. **b.** By replacing the focused laser beam with a Bessel beam, which has a near-infinite depth of focus, there is no need anymore to precisely focus the laser beam onto the cell membrane, thus offering higher throughput.

4.2 Nanoparticle mediated laser-induced photoporation

Direct photoporation requires tight focusing of the laser beam to obtain a sufficiently high photon density for creating a hole in the cell membrane. In combination with light sensitizing nanoparticles, however, a broad laser beam with low photon density can be used instead, thus offering much higher throughput. As illustrated in Figure 7a, in this approach cells are first incubated with sensitizing nanoparticles, e.g. gold nanoparticles, properly functionalized to bind to the cell membrane. Next, laser irradiation is applied to generate photothermal effects by

the nanoparticles that locally enhance membrane permeability. The most common photothermal effects are either heating of the formation of vapor nanobubbles (VNBs) by the rapid evaporation of water surrounding the particles.[87] Especially the latter effect has attracted quite some attention in the past years, as it can be efficiently generated with (less expensive) ns pulsed lasers.[87, 98, 99] Upon absorption of a laser pulse, the induced vapor layer around the sensitizing NPs rapidly expands (10-1000 ns) and collapses, releasing a localized mechanical force that disrupts the cell membrane.[100]

Gold nanospheres (NSP) and nanoshells (NS) were used as sensitizing nanoparticles for forming VNB by 70 ps pulsed laser light to deliver FITC-dextran (FD) into the CD3-positive Jurkat cells by the Lapotko group.[101] Later on, also Xiong *et al.* delivered different sizes of labeled dextrans in different cell lines using 70 nm gold NSPs with 7 ns pulsed laser light, reaching efficiencies of more than 90%.[102] The same was done for functionalized quantum dots (QDs), for which it was shown that asymmetric division of QDs over daughter cells can be avoided by direct cytoplasmic delivery. Xiong *et al.* also demonstrated fast spatial-selective delivery of fluorescent probes, creating intricate labeled patterns in cell cultures and even single-cell transfections.[103] The same group next used this possibility to deliver labels in individual neurons allowing to study their morphology in great detail.[104] Instead of gold nanoparticles, which easily fragment upon laser irradiation, graphene quantum dots (GQDs) were used as more stable sensitizers in more recent work.[105] The GQD being more resistant to pulsed laser irradiation allowed repeated photoporation of cells and careful control of the amount of labels delivered into the cells. It was demonstrated that a broad range of labels could be delivered into cells this way, including phalloidin, SNAP-tag ligands, and fluorescently labeled NPs.

Nanoparticle enhanced photoporation offers several convenient features, including high delivery efficiency over a broad range of molecular sizes, high cell viability, high-throughput

(up to ~100000 cells per second), and compatibility with both adherent and suspension cells. Importantly, being a laser-based technology, it is readily compatible with light microscopy and the typical cell recipients used for that, which is ideal for intracellular labeling. However, there are still plenty of challenges remaining. First, while molecules up to 500 kDa have been shown to be successfully delivered in cells, the efficiency goes down for larger molecule sizes. This is due to a combination of slower diffusion and a steric hindrance at the pores. In addition, metallic NPs, such as AuNPs, tend to fragment upon pulsed laser irradiation. This creates some concern for in vivo applications of cells labeled this way since it has been shown that very small gold nanoparticles can interact with the DNA in cells, thus increasing the chance for genotoxicity.[106, 107] While particle fragmentation has been shown to be avoided by using a femtosecond pulsed laser at an off-resonance wavelength,[108, 109] a more practical approach is likely the use of other photothermal materials that are more photostable, like graphene-based materials, or provide better biocompatibility.[105] A final practical limitation is that nanoparticle enhanced photoporation is not yet commercially available, so that its use remains limited to specialized groups at the moment.

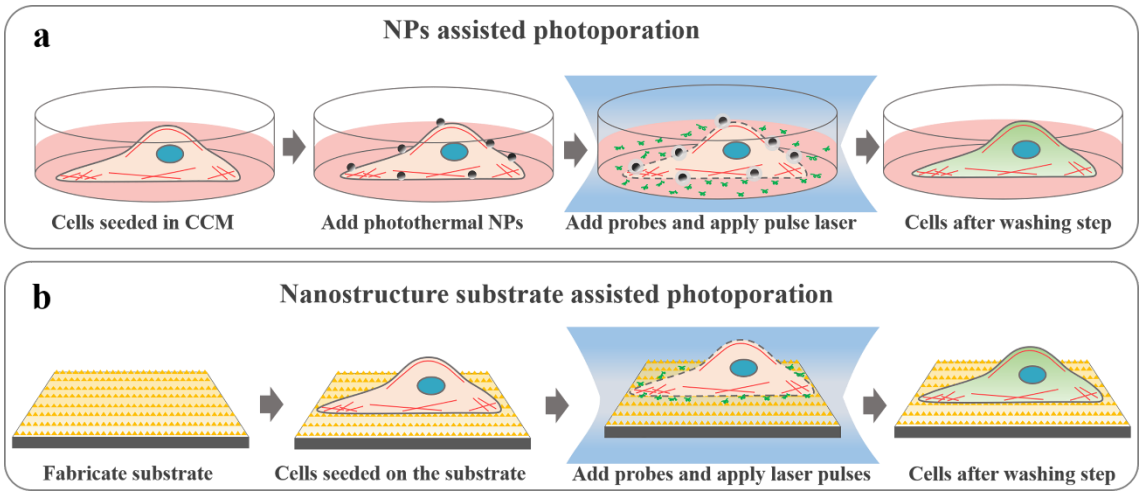

Figure 7. Schematic illustration of laser-induced photoporation with photothermal nanoparticles or substrates. **a.** In nanoparticle assisted laser-induced photoporation, cells are first seeded in a normal cell culture substrate followed by incubation with photothermal NPs. After laser irradiation, fluorescent probes in the cell medium can enter the cytoplasm through transient membrane pores that are created by the nanoparticle's photothermal effects. After

washing labeled cells are obtained. **b.** In nanostructure assisted photoporation, substrates are created with localized photothermal features. Cells are seeded on the substrate, followed by pulsed laser treatment with probes already present in the cell medium. Pores are created in the cell membrane by photothermal effects, allowing probes to enter the cytoplasm. After washing labeled cells are obtained.

4.3 Nanostructure substrate mediated laser-induced photoporation

Instead of adding sensitizing nanoparticles to cells, it is also possible to integrate photothermal features in specially designed substrates onto which cells can be grown or at least collected for treatment (Figure 7b). Upon laser irradiation pores can again be formed in the cell membrane where it is in contact with those photothermal features, allowing the influx of labels that are present in the surrounding cell medium. For instance, Wu *et al.* developed a biophotonic laser-assisted surgery tool (BLAST), being a substrate with an array of micrometer-wide SiO_2 holes coated with crescent-shaped titanium (Ti) thin films (Figure 8a).[110] Membrane pores are generated by microcavitation bubbles from the Ti coating after nanosecond laser irradiation and cargos are delivered into cells by pressure-driven flow through the vertical channels in the silica chip. FITC-dextran (40 kDa) was efficiently delivered into HeLa cells and two other primary mammalian cells with more than 90% cell viability. A similar substrate was fabricated by Madrid *et al.* who achieved 78 % calcein green positive cells with 87% cell viability (Figure 8b).[111] Lyu *et al.* developed a flat substrate with an immobilized gold nanoparticle layer suitable for irradiation by an 808-nm CW laser (Figure 8c).[112] Tetramethylrhodamine isothiocyanate (TRITC)-labeled dextran (4.4 kDa) was delivered into cells with high viability. A similar platform was built by the same group replacing gold nanoparticles with magnetic iron oxide nanoparticles (Figure 8d), showing successful intracellular delivery of TRITC-dextran.[113] Saklayen *et al.* fabricated pyramidal nanoheaters with a gold coating (Figure 8e).[114] After irradiation by nanosecond pulsed laser light, a wide range of FITC-dextrans were deliver into cells with high cell viability. Combined with microfluidics and nanofabrication, Messina *et al.* fabricated a gold nanotube array platform for spatially,

temporally, and quantitatively controlled delivery.[115] The cell membrane is porated by the hot electrons after 8-ps 1064-nm laser irradiation, followed by injection of PI through the microfluidic channel underneath the nanotube (Figure 8e).

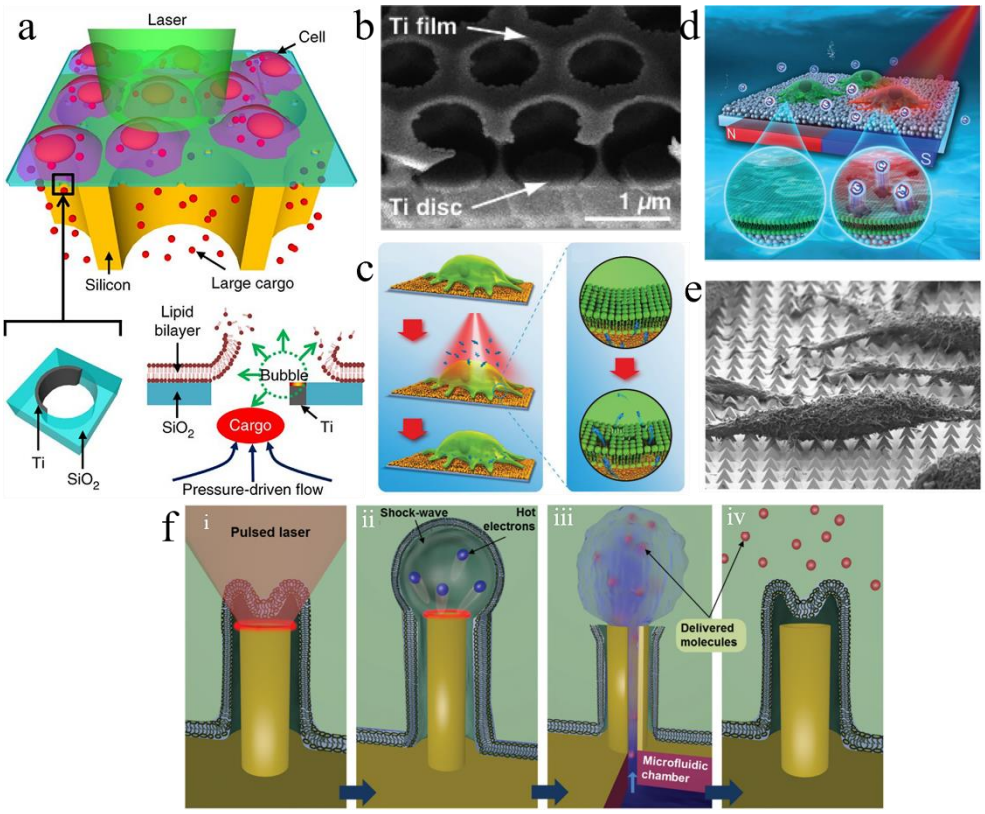

Figure 8. Nanostructure assisted laser-induced photoporation substrates. **a.** The BLAST platform consists of an array of trans-membrane holes patterned on a 1.5-μm-thick SiO_2 film. Crescent-shaped titanium films are asymmetrically coated on the side walls of these holes to absorb the laser energy. Pulsed laser irradiation triggers cavitation bubbles that disrupt the contacting cell membranes. After membrane disruption, an external pressure source is applied to deform the bottom flexible poly(dimethylsiloxane) storage chamber to push cargo into the cytosol of cells via these transient membrane pores. Reproduced from Wu *et al.*[110] and produced with permission from Springer Nature. **b.** Fabrication and characterization of self-assembled thermoplasmonic nanocavity substrates. A tilted scanning electron microscopy (SEM) image of nanocavities show the continuous porous Ti film on top of the nanocavities and disconnected Ti discs at the bottom. Reproduced from Madrid *et al.*[111] produced with permission from the American Chemical Society. **c.** Schematic illustration of macromolecular delivery into living cells grown on gold nanoparticle layer surfaces upon laser irradiation. Reproduced from Lyu *et al.*[112] produced with permission from John Wiley and Sons. **d.** Schematic illustration of using porous magnetic iron oxide nanoparticles as a photoporation nanoplatform for macromolecular delivery. Reproduced from Wang *et al.*[113] produced with permission from Royal Society of Chemistry. **e.** Cells are seeded on the pyramidal nanoheater platform covered with a gold coating. The SEM image shows HeLa CCL-2 cells on the thermo plasmonic substrate. Reproduced from Saklayen *et al.*[114] produced with permission from the American Chemical Society. **f.** Schematic illustration of golden plasmonic nanotubes that are connected to a microfluidic channel underneath. Cells are cultured on top of the array of

plasmonic nanotubes. To deliver compounds into the cells a) a laser pulse is exploited to excite the nanotube, b) pressure waves from a vapor nanobubble are able to locally form pores in the cell membrane, c) molecules are delivered from the microfluidic channel to the intracellular compartment through the nanopore, d) after which the membrane spontaneously closes in few minutes. Reproduced from Messina *et al.*[115] produced with permission from John Wiley and Sons.

Compared to nanoparticle sensitized photoporation the nanostructure substrates have the advantage that they – at least in some cases – avoid direct exposure of cells to nanoparticles. This is an aspect that is especially attractive when labeled cells would need to be imaged in humans, such as for the follow-up of cell-based therapies. Another advantage is that in some embodiments continuous wave (CW) irradiation was already efficient in forming pores, which is of practical and economical interest as they are typically less expensive than pulsed lasers. The downsides are evidently that it requires the fabrication of specialized substrates, often by cleanroom microfabrication technologies which are not readily accessible or may be difficult to scale up. Another difficulty is that cell cultures will need to be optimized for these atypical substrates and that many of them are not transparent, and therefore not easily compatible with light microscopy applications.

5. Micro- and nanoinjection

Microinjection can be considered to be the first physical intracellular delivery method as it uses a fine capillary to puncture the cell membrane. Since its invention in 1911,[116] it has been widely used to bring materials inside cells, primarily for gene delivery,[117-119] but to some extent as well for the intracellular delivery of probes. By microinjection it is possible to deliver almost any kind of probe, irrespective of its size in well-controlled quantities. For instance, PEG-coated QDs were delivered into cells by microinjection, showing bright and homogenous labeling, outperforming the quality obtained with electroporation or biochemical transfection methods[2] Single wall carbon nanotubes (SWCNTs) were also injected into a well-established embryogenesis 3D model as an intracellular label to explore their effects on

embryogenesis.[120] However, microinjection remains a challenging procedure, especially when working with very small cells or suspension cells. Combined with very low throughput, its use will remain limited to dedicated single cell experiments.

To achieve a more gentle contact with the cell membrane, microinjection was recently combined with laser-induced photoporation. The micropipette tip was coated with a light-absorbing titanium thin-film so as to form VNB by irradiation with a nanosecond pulsed laser (Figure 9a).[121, 122] In this way, the micropipette tip no longer had to puncture the cell membrane, but only needed to be brought in close proximity of the cell membrane so that the laser-induced VNB could locally form a pore. Next, the compounds of interest are ejected from the capillary in close proximity to the cell, from where they can diffuse into the cell. Thanks to the relatively large glass capillary pipet, QDs functionalized with tubulin could be delivered into living cells to label tubulin structures. More gentle treatment was achieved by Hennig *et al.* as well who used a nanopipette-assisted electrophoretic delivery method, called nanoinjection (Figure 9b).[123] Compared to a traditional micropipette, the nanoscale size of the pipette is much less harmful to the cells. Integrated with both laser-induced photoporation and electroporation, an ultrashort laser pulse was irradiated on the 100-nm gold-coated nanopipette to disrupt the cell membrane, followed by the delivery of charged fluorescent probes by electrophoretic forces. A number of functionalized fluorescent probes were able to be delivered into different types of living cells for superresolution imaging. When comparing a 100-nm pipette with one of 500-nm diameter, it was found that the smaller-sized pipette induced higher cell survival rate and better cell proliferation after nanoinjection (Figure 9c).[124] Integrated with microfluidics and electroporation, the cells were first trapped in the microchannel. With the assistance of an electric field to form pores in the membrane, the red fluorescent protein (RFP) was manually injected into the trapped cell with a nanochannel (Figure 9d).[125] RFP was controllably delivered this way into several different cell types.

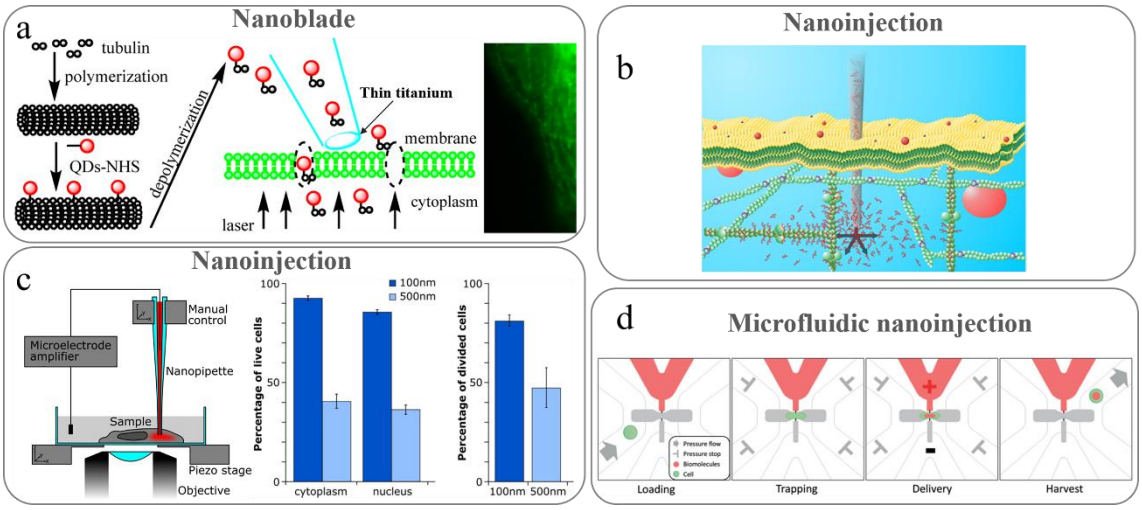

Figure 9. Schematically illustration of different nanoinjection examples. **a.** Photohthermal nanoblade to deliver tubulin−QD conjugates into living cells. The thin titanium coated on the tip of a glass capillary pipet was irradiated by a pulsed laser to make pores in the cell membrane. Reproduced from Xu *et al.*[121] and produced with permission from American Chemical Society. **b.** Principle of nanoinjection to deliver QDs. Using a nanopipette with a diameter of ~100 nm filled with functionalized fluorescent probes, single living cells can be specifically labeled. The ionic current between two electrodes, one placed inside the pipet and the other one placed in the bath, could be used to release the loaded probes. Reproduced from Hennig *et al.*[123] and produced with permission from the American Chemical Society. **c.** Schematic illustration of the nanoinjection platform (left) and cell viability/proliferation results 24 hours after the injection of dextran-Alex Fluor 647 with a 100 nm and 500 nm pipette into the nucleus and cytoplasm. Reproduced from Simonis *et al.*.[124] **d.** A schematic illustration of the microfluidic nanoinjection system. From left to right: loading cells into the cell loading channel, trapping a single cell in the nanoinjection structure, electroporation for protein delivery, and release of the injected cell via the cell-harvesting channel. Reproduced from Yun *et al.*[125] and produced with permission from the Royal Society of Chemistry.

Even though nanoinjection offers better cell viability than traditional microinjection, it still inherently is a fairly slow single cell manipulation technique. At present, it seems unlikely that it will become a general usable technology for delivering probes to a substantial amount of cells. But for proof of concept studies with new types of probes or for dedicated single cell studies micro- and nanoinjection will remain excellent tools to work with.

6. Micro- and nanostructure induced cell membrane disruption

The application of shear forces is another approach to induce membrane permeability. Since the cell membrane is composed of a phospholipid bilayer which is only ~4 nm thick, it is fairly easily mechanically distorted. Shear forces can be applied to cells by specially engineered

micro- or nanostructures on substrates or in microfluidic devices (Figure 10), as discussed below.

6.1 Nanoneedles and nanostraws

The application of shear forces is another approach to induce membrane permeability. Since the cell membrane is composed of a phospholipid bilayer which is only ~4 nm thick, it is fairly easily mechanically distorted. Shear forces can be applied to cells by specially engineered micro- or nanostructures on substrates or in microfluidic devices, as discussed below.

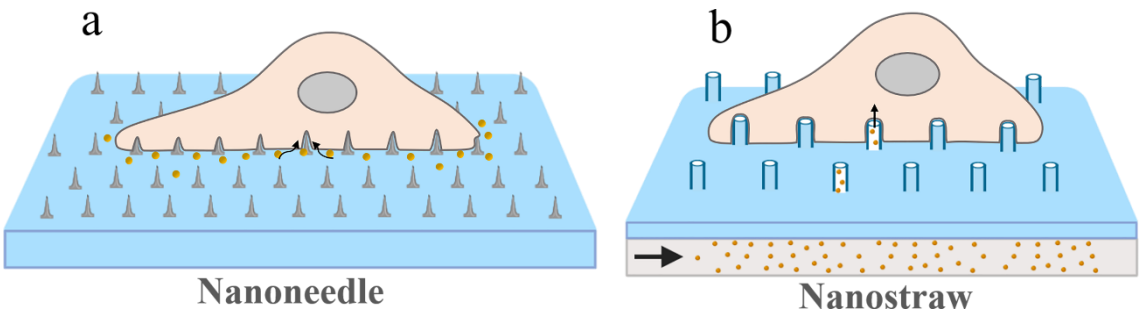

Figure 10. Schematic illustration of cells interacting with an **a.** Nanoneedle and **b.** Nanostraw array platform. Probes that need to be delivered into the cells are indicated by the yellow dots. In the Nanoneedle array, the probes are added to the cell culture medium and will diffuse passively through the pores that are created at the needle tips by shear forces. In the case of the Nanostraw array, the probes are present in a chamber below the substrate and will diffuse into the cells through the hollow nanostraws. Created with BioRender.

Different intracellular probes or labels were successfully delivered into cells using nanoneedle or nanostraw substrates. Chen *et al.* delivered luminescent iridium (III) polypyridine complexes into the cytosol and even into the nucleus by a diamond nanoneedle array with high cell viability (Figure 11a).[126] Wang *et al.* used centrifugation to push a nanoneedle array on top of cultured cells in order to poke the cell membrane (Figure 11b), thus delivering different probes like EthD-1, FITC-dextran, QDs, labeled antibody, and polystyrene nanoparticles, into different types of living cells, including fibroblast cells and hippocampal neurons.[127] The nanostraw platform was used to efficiently introduce the cell-impermeable bioorthogonal probes for cellular studies (Figure 11c).[128] The same group delivered Co^{2+} through the nanostraws to quench the expression of green fluorescent protein (GFP), allowing them to quantify the

percentage of cell membrane penetration.[129] Others developed a biodegradable nanoneedle array for delivery of 6 nm hydrophilic QDs into cells for further *in vivo* studies (Figure 11d).[130, 131]

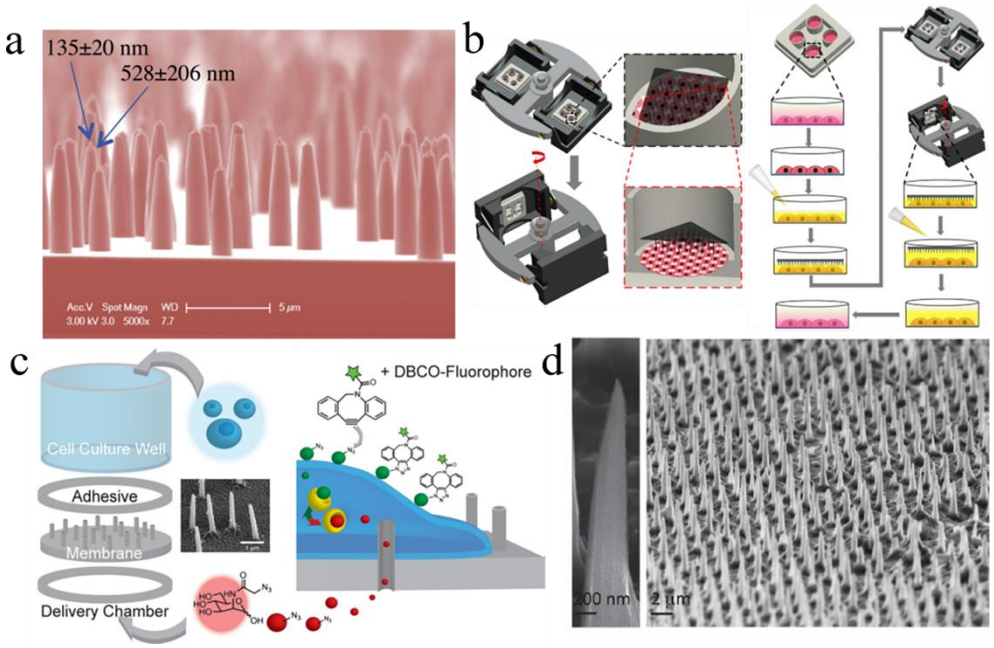

Figure 11. Nanoneedle, nanostraw and nanotube intracellular delivery platforms. **a.** SEM image of diamond nanoneedles for intracellular delivery. Reproduced from Chen *et al.*[126] and produced with permission from John Wiley and Sons. **b.** Schematic illustration of the basic design and working principle of a nanoneedle array-based intracellular delivery system (left). The work flow of the delivery procedures using nanoneedle arrays (right). Briefly, the cell culture medium was first replaced with the basal medium containing the materials to be delivered. The nanoneedle patch was then placed on the cells and centrifuged at various speeds. After centrifugation, extra basal medium containing the delivery material was immediately added to the culture well to lift off the nanoneedle patch. After 5–30 min incubation at 37 °C, the basal medium was washed away and replaced with fresh cell culture medium. Reproduced from Wang *et al.*[127] and produced with permission from Springer Nature. **c.** Nanostraw device used for azidosugar delivery. The device consists of four parts: the cell-culture well, an adhesive layer, the nanostraw membrane, and a delivery chamber (left). The cargo passes directly into cells through penetrating nanostraws. Upon successful entry into the cell, an azidosugar such as ManNAz is enzymatically converted into sialic acid groups and incorporated onto cell-surface glycoproteins (right). These groups retain the azide moiety, which can be specifically labeled with DBCO fluorophore. Reproduced from Xu *et al.*[128] and produced with permission from John Wiley and Sons. **d.** SEM image of a uniform array of conical porous Si nanoneedles, with a <100 nm tip diameter, 600 nm base diameter, 5 μm length, and 2 μm pitch. Reproduced from Chiappini *et al.*[130] and produced with permission from the American Chemical Society.

Although nanoneedles or nanostraws have been used successfully to deliver different probes into cells, the exact mechanism of how the nanoneedles disrupt the cell membrane is still

unknown. A two-step mechanism has been proposed. First “impaling” happens as cells land onto the bed of nanoneedles, after which “adhesion-mediated” penetration occurs when the cells spread and adhere to the substrate.[132] However, others have claimed that the cell membrane remains intact without penetration by the nanoneedles.[133, 134] According to this view the cell membrane engulfs the nanoneedles without contacting the cell interior. Due to the high membrane curvature at the tips, clathrin-mediated endocytosis was found to be stimulated.[135, 136] Therefore, stimulated endocytosis rather than direct cytoplasmic delivery could explain the low delivery efficiencies observed with such nanoneedle substrates.[137, 138] This is supported by the finding that only ~7% of hollow-tube nanowires were actually penetrating the cell membrane.[129] To improve the delivery efficiency, an external force could be added to deform the cell membrane further, such as by centrifugation-induced supergravity or by piezoelectric-driven oscillation.[127, 139] Interestingly, when penetration is achieved, hollow needles can be used to actively deliver compounds to the cytoplasm.[115, 128]

The nanoneedle or nanostraw array offers an advanced physical penetration method for intracellular delivery. It was proven that the delivery efficiency, however, was fairly low, unless extra external forces are applied, such as by centrifugation. On the upside, the nanoneedle or the nanostraw array is mostly fabricated on a biocompatible substrate, which is transparent for microscopy. Or in another case, the nanoneedle is integrated into a patch that penetrates the cells from the top side, such as the case in Figure 10b, which is even more flexible for cell labeling applications. Widespread use of such needle-like arrays will depend on whether these nanofabricated substrates will become broadly available or not, and if biologists are willing to replace their tried and tested cell culture substrates for these needle-like platforms.

6.2 Microfluidics

Microfluidics is a technology for manipulating fluids at the micrometer scale, which is often referred to as lab-on-a-chip devices.[140] It has been actively explored for applications in biology and medical research, offering many unique advantages, such as reduced sample consumption, high throughput, and integration of multiple processes.[140, 141] It comes as no surprise that the minute control offered by microfluidics devices has been leveraged for fast and reproducible permeabilization of the cell membrane as well, including for the delivery of probes. Even though different approaches have been developed (Figure 12), they all rely on the controlled deformation of cells so as to apply shear forces to the cell membrane that make it temporarily more permeable, such as squeezing cells through narrow constrictions, letting cells collide with a sharp tip, or using shear forces induced from the fluid flows themselves.

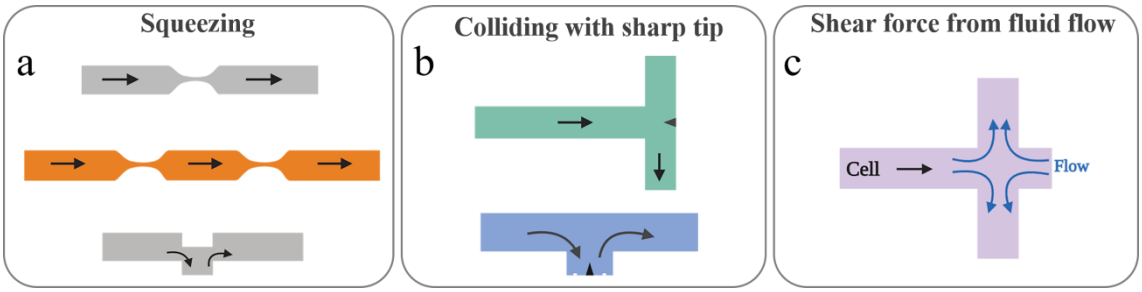

Figure 12. Three different approaches based on microfluidics to permeabilize cells by shear forces. **a.** The cell squeezing approach relies on letting cells flow through one or more narrow constrictions which can have different geometries. **b.** Sharp features can be incorporated in various ways into microfluidic channels onto which cells can collide to locally puncture the cell membrane. **c.** Microfluidic flows can be designed to have regions where high shear forces are exerted to cells which can lead to their permeabilization. In this example two opposing flows come together in a junction of channels, resulting in a flow profile as indicated by the blue arrows. Cells moving into this junction will become stretched and permeabilized by the fluid shear forces, after which they will move towards an outlet through the upper or bottom channel. Created with BioRender.

The most common way is by flowing cells through microchannels that one or more narrow constrictions with a dimension smaller than the cell size. Due to friction with the channel walls at the constriction site transient pores in the cell membrane are created, a process that has become known as cell squeezing (Figure 12a and 13a). Sharei *et al.* fabricated multiple parallel microfluidic channels on one chip with constrictions being 4 to 8 µm wide and from 10 to 40

μm long. With this system, 3 and 70 kDa dextran were successfully delivered into multiple cell types at a throughput rate of 20,000 cells/s.[142] In addition, they showed successful delivery of 15-nm AuNP, QDs and antibodies. Lee *et al.* fabricated similar microfluidic channels with a constriction width of 6 μm to deliver QDs (hydrodynamic size ~13 nm) into living HeLa cells, reaching 35% efficiency with > 80% cell viability.[143] This approach was later used by Kollmannsperger *et al.* for the delivery of small fluorescent molecules into living cells for protein visualization with superresolution microscopy.[144] In another study, Klein *et al.* used cell squeezing to deliver nanobodies into living cells for microscopy imaging.[145] To further increase the efficiency of probe delivery, two sequential constriction sites have been used as well for double membrane permeabilization (Figure 13b).[146] In this way, 80 % of cells were successfully labeled with TRITC 2000 kDa. Along the same line, a design with two sequential deformation sites with different geometries was fabricated by Modaresi *et al.* to create pores at different locations in the cell membrane (Figure 13c), thus increasing the number of positive cells.[147] Additionally, they also designed a dispersion zone prior to the squeezing channels to efficiently prevent the formation of cell agglomerates, a strategy which was also used in another study.[148] With FD3 and FD70 it was demonstrated that the delivery efficiency of the double constriction design was superior to a single deformation modality.

While the principle of cell squeezing has been amply demonstrated to offer efficient cell delivery of all kinds of extrinsic molecules, it is clear from its concept that it needs careful optimization of the constriction dimensions per cell type. While this limitation has been cleverly used to demonstrate size-selective intracellular delivery from a heterogeneous mixture of cells,[149] for general use as a delivery platform it is a critical drawback, which is further complicated by frequent clogging of the system.[149] To overcome these limitations, Deng *et al.* created an alternative design, termed the inertial microfluidic cell hydroporator (iMCH), in which shear forces are applied to cells by letting them collide with a sharp tip at a T-junction

(Figure 11b and 12d).[150] Aided by local enhanced fluid-shear this induced membrane disruption allowing macromolecules to enter the cells. More than 80 % of positive cells were successfully labeled with FD3 with cell viability > 90 %. Following a similar concept, cell membrane disruption was also achieved by Dixit *et al.* on a microfluidic platform that first aspirates cells onto a sharp tip, after which the flow direction is reversed to release the punctured cell (Figure 13e).[151] Although they did not apply this platform for intracellular label delivery, successful plasmid DNA delivery indicated that it could be used for that purpose as well, even with large-sized labels. In another approach, cells were permeabilized by the fluid streams themselves, such as the hydroporator that was developed by Kizer *et al.* (Figure 11c and 12f).[152] It demonstrated high delivery efficiency with 3-5 kDa FD and high cell viability, with the possibility to deliver large molecules up to 2000 kDa into cells.

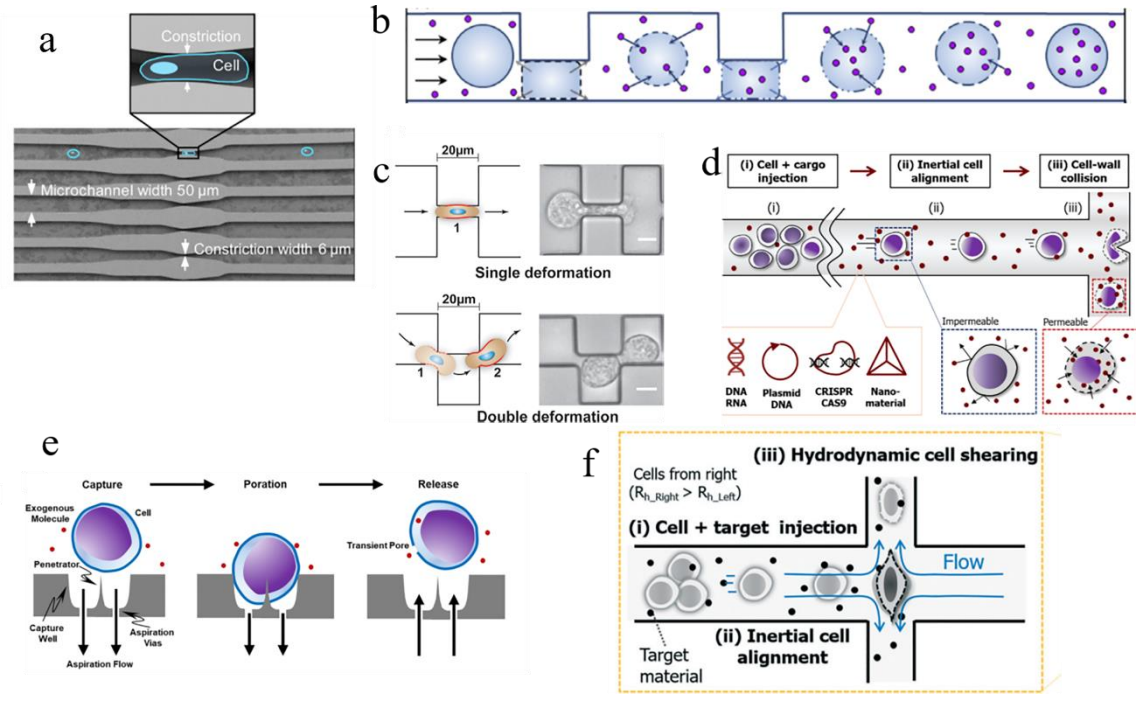

Figure 13. Microfluidics platforms for intracellular delivery of probes. **a.** Delivery mechanism and system design of multiple parallel microfluidic channels. The inset shows a magnified view of a constriction site through which cells are flown. Reproduced from Sharei *et al.*[142] and produced with permission from PNAS. **b.** The cross-sectional view of a cell undergoing compression under two sequential ridges. Reproduced from Liu *et al.*[146] and produced with permission from Elsevier. **c.** Schematic illustration and microscopy image comparing cell squeezing with two different deformation modalities. In the double deformation method cells are permeabilized two times rather than one time in the single deformation method (scale bar =

10 μm). Reproduced from Modaresi *et al.*[147] and produced with permission from John Wiley and Sons. **d.** Schematic illustrating the design and operating principles of the inertial microfluidic cell hydroporator (iMCH) for the intracellular delivery of nanomaterials. Cell-wall collision and fluid-shear stress create nanopores in the cell membrane, allowing external molecules to diffuse through. Reproduced from Deng *et al.*[150] and produced with permission from the American Chemical Society. **e.** Cells are flown towards a sharp tip by which they become punctured, after which they are released again by reversing the flow. Reproduced from Dixit *et al.*[151] and produced with permission from the American Chemical Society. **f.** Schematic illustration of the design and operating principles of the hydroporator device that permeabilizes cells by fluid shear forces at a cross-sectional junction with opposing flows. Reproduced from Kizer *et al.*[152] and produced with permission from the royal society of chemistry.

The major advantage of these microfluidic devices is that they combine high delivery efficiency with extremely high throughput. It is an added advantage that the sample volumes are inherently small, which is especially attractive when working with expensive labels, such as quantum dots or labeled nanobodies. A practical limitation, on the other hand, is that cells need to be in suspension during the labeling process, limiting its practical use at least for microscopy imaging which is often performed on adherent cells. Other drawbacks, as mentioned above, are that new optimized designs are generally needed for each cell type and that devices may suffer from clogging. For labeling cells for *in vivo* cell tracking, this is, however, an attractive option to look into.

7. Nanomachines

Nanomachines or nanomotors, also termed nanorobots or nanovehicles, are miniature devices that convert diverse sources of energy into movement or force, in such a way that allows them to displace in conditions of low Reynolds numbers and at the same time to have a preferential directionality overcoming the Brownian motion.[153] Recently they have been explored for intracellular biosensing and targeted delivery.[154, 155] The energy needed to induce actuation may come from chemical reactions at their surface which due to asymmetry in the composition generates local concentration gradients, an electrical potential or gas bubbles that drive them forward.[153] Alternatively, asymmetry in the morphology of the nanomachines allow them to

use external stimuli as the energy source to initiate the motion, including magnetic, ultrasound (US), optical, thermal and electrical energy.[156-158] To achieve intracellular label delivery, labels are either loaded on the nanomachines or co-delivered to the cell medium for diffusion into cells after membrane poration.

In order to enter the cell interior, the powerful physical external energies like ultrasound (US) and magnetic fields are preferable to propel nanomachines more vigorously. Gold nanowire nanomotors (AuNW) are the most used nanomotors that are propelled by the external US or magnectic field to penetrate into cells. Conjugated with dye-labeled single-stranded DNA (ssDNA)/graphene-oxide (GO), the AuNW nanomotors achieved intracellular "OFF-ON" fluorescence switching for intracellular biosensing (Figure 14a).[159, 160] Propelled by US, the nanomotor was able to penetrate into cells to let the ssDNA hybridize with miRNA-21, thus dequenching the fluorescent dye and labeling the miRNA-21 molecules. This approach was used for the rapid monitoring of miRNA-21 expression in individual intact cancer cells. With the same delivery system, the Cas9/sgRNA complex loaded nanomotor was delivered into cells by US for GFP knockout.[161] The synthetic nanoswimmer, as one type of the nanomachines, has attracted a lot of attention for gene and drug delivery.[162, 163] Based on different propulsion energy, there are normally US and magnetic field propelled nanoswimmers.[164-166] As a carrier for intracellular delivery, nanospears coated with gold, loaded with plasmid DNA, were developed by Xu *et al.* that could be propelled to the cells by a magnetic field (Figure 14b).[163] Although it was only applied for gene delivery, one can imagine that it could be used for intracellular probe delivery as well. Although the US or magnetic field is used to propel the nanomachine to enter the cells, however, the intracellular entry is difficult to be realized by mechanical opening the cell membrane. This is because the maximum applied stress of these nanoswimmers is still smaller than the critical ruptured stress of the cell membranes.[163] Therefore, combined strategies are being explored to actively porate the cell

membrane, by the combination of nanoswimmer with powerful cell-membrane permeabilization method. An example of this is the use of laser-induced heating for cell membrane poration integrated with the nanoswimmer for intracellular delivery. In this approach, Wang *et al.* used an ultrasound-driven tubular gold-nanoshell (AuNS) nanoswimmer functionalized with a polymeric multilayer for the photomechanical opening of the cell membrane by NIR laser irradiation (Figure 14c).[167] The acoustical power allows the nanoswimmer to move to the cell membrane, while the AuNS converts the NIR laser energy into heat to locally disrupt the cell membrane. Membrane disruption was successful in this way as evidenced by an influx of PI present in the cell medium. Instead of inorganic nanomaterials, also protein-based molecular motors are considered as one type of nanomachine that can open the cell membrane by changing their conformation in a controlled manner in response to external stimuli, like laser light. Organic molecules could change their conformation upon external stimuli to pass through the lipid bilayer, while also to be the fluorophore to label the cells. García-López *et al.* designed and synthesized molecular motors that could penetrate the membrane bilayer upon activation by UV laser irradiation (Figure 14d).[168] Fluorescent molecules could then enter the cytosol and label intracellular structures. Cell viability was as high as 90% after the treatment.

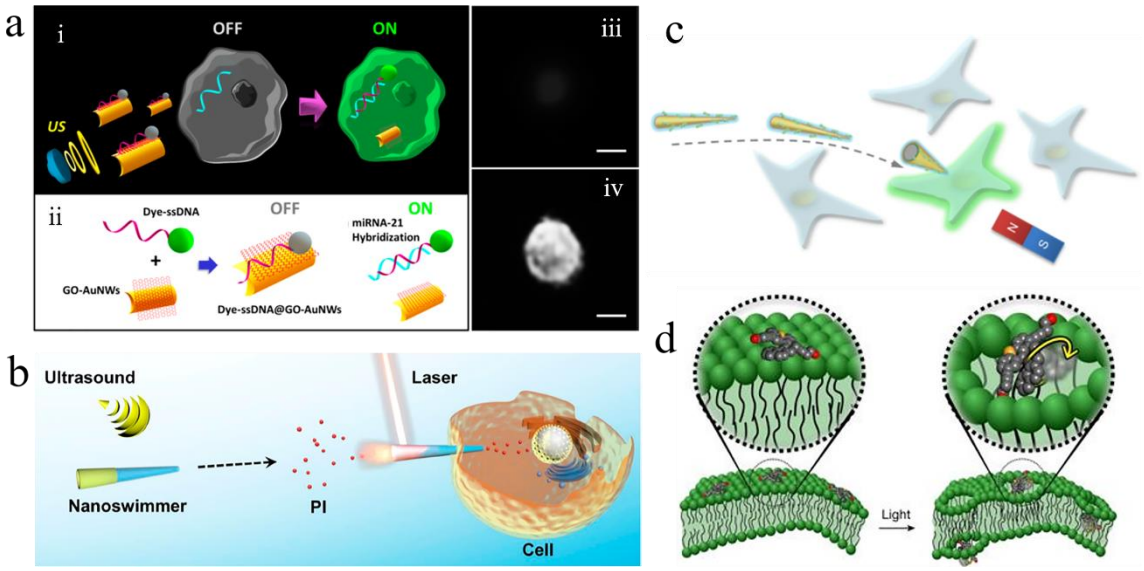

Figure 14. Different nanomachines for intracellular labeling. **a.** Intracellular detection of miRNAs by US-propelled ssDNA@GO-functionalized gold nanomotors. Schematic illustration of (i) the "OFF-ON" fluorescent switching system for specific detection of miRNA-21 in intact cancer cells, and (ii) the sequential steps involved: immobilization of the dye-ssDNA on the GO-functionalized AuNWs and quenching of the dye fluorescence, and fluorescence recovery due to release of the dye-ssDNA from the motor's GO-quenching surface upon hybridization with the target miRNA. Fluorescence images of a MCF-7 cell (iii) before and (iv) after 20 min incubation with the ssDNA@GO-modified AuNWs while being exposed to US stimulation. Scale bar, 10 μm. Reproduced from Avila *et al.* and produced with permission from the American Chemical Society. **b.** Schematic cell poration of polymer AuNS-functionalized nanoswimmers upon exposure to NIR light. Reproduced from Wang *et al.*[163] and produced with permission from the American Chemical Society. **c.** Schematic illustration of Si/Ni/Au nanospears that become inserted into a target cell by magnetic propulsion to deliver a GFP-plasmid. Reproduced from X. Xu *et al*[167] and produced with permission from the American Chemical Society. **d.** Schematic illustration of a molecular machine interacting with a cell membrane (left). The membrane is then opened by UV-activated nanomechanical action. Reproduced from García-López *et al.*[168] and produced with permission from Springer Nature.

Propelled by external energy, the nanomachines could achieve active intracellular delivery. As they are still in a very early explorative phase, it remains uncertain what their future role will be to deliver labels into cells for actual applications. Nevertheless, the nanomachines are a fantastic demonstration of what is currently possible with nanotechnology and certainly deserve further exploration, including for cellular labeling purposes.

Discussion

Most of the intracellular delivery approaches that we have reviewed here were originally developed for drug and gene delivery, but have been proven to be useful for the intracellular delivery of other types of compounds as well, including probes which are crucial for investigating (intra)cellular dynamics. It is of interest to consider the various methods in terms of their strengths and weaknesses according to several aspects, including throughput, compatibility with microscopy, suitability for adherent or suspension cells, compatibility with different cell types and different types of probes, limitations inherent to the method and practical limitations. Our assessment of the probe delivery technologies according to these aspects is listed in Table 1. As mentioned before, it is attractive to consider the repurposing of drug delivery nanocarriers for the intracellular delivery of probes since many types are already

available and they are relatively inexpensive and easy to use. However, as it is well-known in the drug delivery field, they suffer from very limited endosomal escape after endocytic uptake. Even though endosomal sequestration of labels can cause quenching and label degradation, this may not be a limiting factor for labeling of whole cells, as is for instance needed in (in vivo) cell tracking applications. However, when the aim is to visualize subcellular structures by microscopy, sequestration of labels in endosomes will result in a confounding staining pattern. As such we consider them less ideal for microscopic investigations of subcellular processes. The same is true for CPPs as well, which are often believed to directly penetrate the cell membrane, but in practice are frequently taken up by endocytosis, especially after conjugation to (large) cargo molecules. As such it seems preferable for labeling applications to look for delivery methods that avoid endocytic uptake and instead provide direct access to the cytosol. SLO, is such a biochemical approach that creates pores in the plasma membrane through which compounds up to ~150 kDa can diffuse into cells. As a biochemical compound it can be easily applied to cells, but the dose and duration of SLO treatment need to be strictly controlled in a cell-type dependent manner to avoid too much toxicity.

Physical delivery methods offer an alternative route to increase the permeability of the cell membrane. Compared to biochemical strategies they tend to be more universally applicable to different cell types and types of probes. Electroporation is likely the most well-known physical delivery method. While bulk electroporation can only be applied to cells in suspension and is often associated with high acute cytotoxicity, newer forms are emerging that offer the possibility to treat adherent cells as well. General access to these new and enhanced forms of electroporation is, however, limited at present since they rely on micro/nanofabrication, which is not readily accessible to the general biomedical researcher. In addition, the reported electroporation substrates are not easily compatible with light microscopy as not all of them are transparent. Instead of electricity it is possible to use light as well as a physical trigger to

enhance cell membrane permeability. With direct photoporation, a high energy pulsed laser is used to create holes in the cell membrane, one at a time. While very efficient for the delivery of even very large compounds, it has a low throughput and is being replaced by newer forms that rely on nanotechnology to enhance photothermal effects. A straightforward approach is the use of photothermal sensitizing nanoparticles which can be easily added to cells. They can induce local cell membrane disruption by laser-induced heating effects or mechanical forces resulting from water vapor bubbles that quickly expand and shrink around the surface of the particle. Plenty of evidence has been provided that this methodology is suitable for the delivery of probes in both adherent and suspension cells, combining high efficiencies with excellent cell viability and extremely high throughput. It has the added advantage that, as an optical technique, it is readily compatible with cell recipients that are traditionally used for optical imaging. One can even imagine that the process could be easily integrated on laser-based microscopy systems. At present, however, since it requires pulsed lasers and dedicated optomechanics to scan large substrates, its widespread use remains limited to specialized groups. As an alternative to sensitizing nanoparticles also substrates have been engineered with photothermal nanostructures onto which cells can be cultured. Compared with NP sensitizer, the specifically designed substrate could achieve active delivery, such as the BLAST. Even though such advanced approaches are even less easily accessible, they may become of future interest for the labeling of cells for *in vivo* tracking applications where one preferably avoids contact between cells and nanoparticles.

Microinjection is another classic intracellular delivery method that uses a micropipette to penetrate the cell membrane and inject the probes actively into the cells. It offers the most precise control but is slow and not easy to handle. Nanoinjection is a more recent variant on the same principle, but with the advantage of being less damaging to cells due to the smaller needle diameter. However, both micro- and nanoinjection have a low throughput due to single-cell

based treatment. Micro- or nanoinjection is expected to remain of interest for smaller proof-of-concept studies of new types of probes or for dedicated single-cell experiments.

Shear stress can be used as well to permeabilize cell membranes, as is the case for nanoneedle substrates and its variants such as, nanostraws or nanotubes. However, unless assisted by an extra external force, like centrifugation, their delivery efficiency as well as throughput remain quite limited to date. In addition, such nanoneedle substrates are not readily available outside specialized groups at the moment. More advanced at present are microfluidics devices that apply shear stress to cells by energetic contact with physical objects or fluid streams. Many promising results have been published over the years with high reported delivery efficiencies and excellent cell viability. This methodology is extremely fast and, once the chip is designed, easy to use. Its limitations are that cells need to be brought in suspension first and the chip design may need to be optimized for different cell types. Likely it has the most promise for labeling specific types of (patient) cells for in vivo cell tracking applications.

The final and most experimental strategy for the intracellular delivery of probes is the use of nanomachines or nanomotors that can actively target the cells and penetrate the cytoplasm. It is a relatively new concept for intracellular delivery, and especially for intracellular labeling. While the technology doesn’t seem very usable yet compared to the other delivery technologies, it is a striking example of what is currently possible with nanotechnology. One can only imagine what their capabilities will be in the not too distant future.

Table 1.1 Comparison of the intracellular delivery strategies discussed in this review

Delivery strategies	Throughput[a)]	Microscopy compatibility	Adherent/ suspension cells	Active/passive delivery	Universality (cell type/probe)	Method limitation	Practical limitation
Nanocarrier	High	Yes	Both	Passive	No	Endocytosis	Sophisticated conjugation/functionalization
CPPs	High	Yes	Both	Mixed	No	Endocytosis	Sophisticated conjugation
PFT SLO	High	Yes	Both	Passive	Probe	Size limit up to 150 kDa	Recover process needed
Bulk electroporation	High	No	Suspension	Passive	Yes	Potential toxicity	Probes aggregation
Adherent electroporation	High	Yes	Adherent	Active	Yes	No flexible substrate	Micro/nanofabrication needed
Direct laser-induced photoporation	Low	Yes	Both	Passive	Yes	Focused pulsed laser needed	Time consuming/expensive laser
NP-mediated laser-induced photoporation	High	Yes	Both	Passive	No	NPs dependent	Hard to access
Nanostructure substrate mediated laser-induced photoporation	High	Yes	Both	Both	No	No flexible substrate	Micro/nanofabrication needed
Micro- and nanoinjection	Low	Yes	Adherent	Active	Probe	Inefficient	Hard to manipulate
Nanoneedles and nanostaws	Low	Yes	Both	Passive	Yes	Exact mechanisms unknown	Micro/nanofabrication needed
Microfluidics	High	No	Suspension	Passive	Probe	Cell size dependent	Clogging potential
Nanomachines	Low	Yes	Adherent	Active	No	Inefficient	Hard to manipulate

[a)] High is defined as ≥ 10000 cells/s, while low is < 1000 cells/s.

Clearly each methodology has its advantages and disadvantages with regard to delivering probes into live cells. The delivery efficiency, the cell viability, the probe size limit, the compatibility for microscopy, throughput and user-friendliness are all aspects to be considered. To help direct the reader to the most suitable technology, Table 1.2 summarizes all these aspects per probe (ordered according to increasing size) as reported in the literature and mentioned in this review.

Table 1. Summary of different intracellular labels from small to large delivered by different strategies in this review

Probes	size	Delivery methods	Efficiency	Throughput	Viability	Application	Adherent/ suspension	Reference
Ions (Ca^{2+}, Zn^{2+})		Direct photoporation (Nd:YAG pulsed laser)	85-100 %	500 cells/ s	80 %	Intracellular study	Adherent	[92]
Sytox Green and Sytox Blue						Cell labeling	Adherent	[92]
Ions (Co^{2+})		Nanostraw	20 %	-[b)]	-	GFP quenching	Adherent	[129]
Ethidium bromide		Direct photoporation (fs pulsed laser)	70-80 %	-	-	Intracellular labeling	Adherent	[94]
			~100 %	-	-	Intracellular labeling	Adherent	[93]
		Direct photoporation (Nd:YAG ps laser)	2.5 %	-	-	Intracellular staining	Suspenstion (Plant cells)	[169]
		Direct photoporation (Bessel beam fs laser)	26.6 %	10 cells/s	high	Intracellular staining	Adherent	[96]
Propidium iondide		Adherent electroporation (nanostraw)	> 95 %	-	high	Cell labeling	Adherent	[82]
		Adherent electroporation (nanotube)		100000/h	high	Cell labeling	Adherent	[115]
		Branched Nanostraw-Electroporation Platform	~ 80 %	-	>95 %	Cell labeling	Adherent	[84]
	≤ 1 kDa	nanoswimmer nanomachine	-	-	-	Intracellular staining	Adherent	[163]
Mito Tracker		Nanoinjection	-	-	-	Microscopy imaging	Adherent	[123]
Sytox Green			-	-	-		Adherent	
Paclitaxel			-	-	-		Adherent	
		Photothermal plasmonic substrates (Ti) with 1064 nm ns laser	78 %	-	87 %	Cell labeling	Adherent	[111]
		Plasmonic substrates (Au) with 1064 nm ns laser	90 %	-	> 90 %	Cell labeling	Adherent	[114]
Calcein green		CB photoporation (1064 nm ns pulse laser)	>80 %	-	>90 %	Cell labeling	Suspension	[170]
		Inverted and upright TiN micropyramids platform (1064 nm, 11 ns pulse)	>83 %	-	-	Cell labeling	Adherent	[171]
SNAP-tag ligand		NPs mediated laser-induced photoporation	>50 %	-	>80 %	Microscopy imaging	Adherent	[105]
tris-N-nitrilotriacetic acid		Microfluidic sqeezing	High	High	High	Microscopy imaging	Suspension	[144]
Azidosugar		Nanostraw	-	-	-	Introcellular study	Adherent	[128]

		AuNP photoporation (561 nm ns pulse laser)	25 %	-	high	Selective delivery	Adherent	[172]
Palloidin, Alex Fluor		Graphene-based electroporation	> 80 %	-	-	Microscopy imaging	Adherent	[86]
		GQD photoporation (561 nm ns pulse laser)	~ 50 %	-	> 80 %	Microscopy imaging	Adherent	[105]
Phalloidin, rhodamine		Direct photoporation (NIR fs pulsed laser)	-	-	-	Specific intracellular labeling	Adherent	[96]
Phalloidin, ATTO 655		Nanoinjection	-	-	-	Microscopy imaging	Adherent	[123]
Gd		CPPs	-	-	-	MRI	Adherent	[58]
FD 0.6 kDa		Thermalplasmonic substrates (Ti) with 1064 nm ns laser	78 %	-	87 %	Cell labeling	Adherent	[111]
Tetramethylrhodamine-dextran	3 kDa	Direct photoporation (Nd:YAG pulsed laser)	85-100 %	500 cells/ s	80 %	Cell labeling	Adherent	[92]
		Microfluidic squeezing	< 50 %	20000 cells/s	< 25 %	Cell labeling	Suspension	[142]
FITC-dextran	3 kDa	Inertial microfluidic cell hydroporator (iMCH)	80 %	>1000000 cells/min	> 90 %	Cell labeling	Suspension	[150]
		Microfluidic squeezing (double deformation)	85 %	high	> 80 %	Cell labeling	Suspension	[147]
FITC-dextran	3-5 kDa	Microfluidics (Hydroporator)	> 90 %	>1600000 cells/min	> 90%	Cell labeling	Suspension	[152]
		Nanoneedle array+ centrifugation	> 80 %	high	~ 95 %	Cell labeling	Adherent	[127]
Tritc dextran 4.4 kDa	4.4 kDa	Porous magnetic iron oxide NPs platform photoporation (808 nm irradiation)	-	-	High	Cell labeling	Adherent	[113]
		Immobilized gold nanoparticle layer for photoporation	-	-	~100 %	Cell labeling	Adherent	[112]
Molecular motors	~1 nm	Molecular motor with UV light	-	-	-	Cell labeling	Adherent	[168]
		Plasmonic substrates (Au) with 1064 nm ns laser	79 %	-	> 90 %	Cell labeling	Adherent	[114]
FITC-dextran	10 kDa	CB photoporation (1064 nm ns pulse laser)	> 80 %	-	> 90 %	Cell labeling	Suspension	[170]
		Direct photoporation (NIR fs pulsed laser)	70 %	-	-	Cell labeling	Embryos cells	[95]
		GQD photoporation (561 nm ns pulse laser)	~ 50 %	-	> 80 %	Microscopy imaging	Adherent	[105]
Iridium (III) polypyridine complex	< 2nm	Diamond Nanoneedle Array	-	-	-	Cell labeling	Adherent	[126]
Dextran, Alexa Fluor 647	10 kDa	Electrophoretic nanoinjection	-	-	> 90 %	Cell labeling	Suspension	[124]

		Streptolysin O	>85 %	-	-	Microscopy imaging	Adherent	[68]
Nanobody	~15 kDa	GQD photoporation (561 nm ns pulse laser)	~ 50 %	-	> 80 %	Microscopy imaging	Adherent	[105]
		Microfluidic sqeezing	High	High	High	Microscopy imaging	Suspension	[173]
QDs	3-4 nm	CPP	95 %	-	-	Cell tracking	Adherent	[55]
Red fluorescent protein (RFP)	26 kDa	Nanoinjection (on microfluidic chip)	< 50 %	high	> 95 %	Cell labeling	Suspension	[125]
Enzymes	29 kDa	Biophotonic laser-assisted surgery tool (BLAST)	> 90 %	~100000 cells/min	> 90 %	Cell labeling	Adherent	[174]
FITC-dextran	40 kDa	Biophotonic laser-assisted surgery tool (BLAST)	> 90 %	~100000 cells/min	> 90 %	Cell labeling	Adherent	[174]
		CB photoporation (1064 nm ns pulse laser)	~60 %	-	> 90 %	Cell labeling	Suspesnion	[170]
		Plasmonic substrates (Au) with 1064 nm ns laser	72 %	-	> 90 %	Cell labeling	Adherent	[114]
		Thermalplasmonic substrates (Ti) with 1064 nm ns laser	< 78 %	-	87 %	Cell labeling	Adherent	[111]
FITC-dextran	70 kDa	Microfluidics (Hydroporator)	~ 73 %	>1600000 cells/min	> 90 %	Cell labeling	Suspension	[152]
		Microfluidic squeezing	< 50 %	20000 cells/s	< 25 %	Cell labeling	Suspension	[142]
		Microfluidic squeezing (double deformation)	54 %	high	> 80 %	Cell labeling	Suspension	[147]
		Inertial microfluidic cell hydroporator (iMCH)	65 %	>1000000 cells/min	> 90 %	Cell labeling	Suspension	[150]
QDs	10 nm	CPPs	Low	-	-	Intracellular tracking	Adherent	[54]
FD 100	100 kDa	Streptolysin O	-	-	-	Cell labeling	Adherent	[67]
		Plasmonic substrates (Au) with 1064 nm ns laser	68 %	-	> 90 %	Cell labeling	Adherent	[114]
FITC-dextran 150	150 kDa	Thermalplasmonic substrates (Ti) with 1064 nm ns laser	< 78 %	-	87 %	Cell labeling	Adherent	[111]
		Microfluidics (Hydroporator)	69 %	>1600000 cells/min	> 90 %	Cell labeling	Suspension	[152]
		Biophotonic laser-assisted surgery tool (BLASTST)	< 50%	~100000 cells/min	> 90 %	Cell labeling	Adherent	[175]
Antibody	150 kDa (20 nm)	Nanoneedle with centrifuge	35.5±4.4 %	high	> 90 %	Cell labeling	Adherent	[127]
		Graphene-based electroporation	> 80 %	-		Microscopy imaging	Adherent	[86]

		Streptolysin O	< 88 %	-		Microscopy imaging	Adherent	[68]
Tubulin-QDs	> 100 kDa	Nanoblade nanoinjection	-	-		Microscopy imaging	Adherent	[121]
		CB photoporation (1064 nm ns pulse laser)	30 %	-	> 90 %	Cell labeling	Suspesnion	[170]
FITC-dextran	500 kDa	Plasmonic substrates (Au) with 1064 nm ns laser	24 %	-	> 90 %	Cell labeling	Adherent	[114]
		Thermalplasmonic substrates (Ti) with 1064 nm ns laser	< 78 %	-	87 %	Cell labeling	Adherent	[111]
		Microfluidics (Hydroporator)	~ 60 %	>1600000 cells/min	> 90 %	Cell labeling	Suspension	[152]
functionalized QDs	~13 nm	AuNP photoporation (561 nm ns pulse laser)	>80 %	-	> 80 %	Long-term labeling	Adherent	[102]
		Microfluidic squeezing	~ 40 %	~10000 cells/s	> 80 %	Cell labeling	Suspension	[143]
AuNPs	15 nm	Microfluidic squeezing	< 50 %	20000 cells/s	> 75 %	Cell labeling	Suspension	[142]
Green fluorescent polystyrene beads	20 nm	Biophotonic laser-assisted surgery tool (BLASTST)	93 %	~100000 cells/min	> 90 %	Cell labeling	Adherent	[175]
QDs	20 nm	Microfluidic squeezing	60%	20000 cells/s	> 75 %	Cell labeling	Suspension	[142]
		Nanoneedle array+ centrifugation	> 80 %	high	< 10 %	Cell labeling	Adherent	[127]
QD-PEG	~ 28 nm	Microinjection	-	-	-	Microscopy imaging	Adherent	[2]
		Electroporation	-	-	-		Suspension	
Gold nanorod	25×90 nm	Adherent elecroporation	-	-	-	NP detection	Adherent	[83]
Single wall carbon nanotubes	147 nm length	Microinjection	-	-	-	Subcellular localization	Embryo model	[120]
Polystyrene NPs	200 nm	Nanoneedle with centrifuge	14.8±2.9 %	high	> 90 %	Cell labeling	Adherent	[127]
Cy5-labeled DNA	0.1-0.5 µm	Bulk electroporation	high	-	-	Single particle tracking	Suspension	[176]
FITC-dextran	2000 kDa	Plasmonic substrates (Au) with 1064 nm ns laser	16 %	-	> 90 %	Cell labeling	Adherent	[114]

		Microfluidics (Hydroporator)	~ 58 %	>1600000 cells/min	~ 75 %	Cell labeling	Suspension	[152]
		Thermalplasmonic substrates (Ti) with 1064 nm ns laser	< 78 %	-	87 %	Cell labeling	Adherent	[111]
TRITC	2000 kDa	Microfluidic squeezing (two compression ridges)	80 %	High	~ 100 %	Cell labeling	Suspension	[146]
Dextran, Alexa Fluor 488	3000 kDa	Nanofountain Probe Electroporation	> 95 %	Low	> 92 %	Cell labeling	Adherent	[85]
Green fluorescent polystyrene beads	2 µm	Biophotonic laser-assisted surgery tool (BLASTST)	62 %	~100000 cells/min	> 90 %	Cell labeling	Adherent	[175]
dye-labeled single-stranded DNA/graphene oxcide/AuNW	>1 µm	nanomachine	-	-	-	Cell real-time sensing	Adherent	[159]

[b] unknown data.

Future perspective

As most of these intracellular delivery strategies are based on passively diffusion, which could induce limitation for delivery of large probes as well as waste of expensive labeling probes. In this end, the active delivery is also important to promote the large probes to enter the cytoplasm, like the biophotonic laser-assisted surgery tool (BLASTST) that uses the pressure flow to drive the cargos into the cells, which can even deliver 2-μm fluorescent polystyrene beads into the cells.(reference) In the case of nanostraw, active delivery could also be achieved by pressure flow from the hollow channel. Based on the fabricated substrates, the compatibility with the high-resolution microscopy after intracellular delivery depends on the transparency and thickness of the substrate. The micro- or nanoinjection could also achieve active delivery, but the low throughput and high complexity of manipulation restrict its widely application. The new arising nanomachines are promising tools for active delivery, but it is still at the starting stage.

As all the delivery strategies in this review are used for cell-impermeable probes, it is also important to choose the suitable probes. As illustrated in Figure 1, different types of intracellular probes are listed in the order of size. For the most common specific labels, organic dyes are the smallest ones, while Abs are the relative larger ones. Both Ab and Nb are cell impermeable, while the protein-tags are intrinsically expressed in genetically modified cells. Still, in case of the tag systems not all fluorescent ligands are cell impermeable, a remark that applies to the organic dyes as well. Considering the size, ease-to-use and costs aspects, for high specific labeling, probably the labeled Nb and organic dyes are the better choices for live cell labeling, but currently there are only limited types of Nbs and organic dyes on the market.

Other than the fluorescent labels, this delivery technique could also help the chemists to deliver the probes into cells as nanosensor, which is useful to explore the intracellular micro- and nano-

environment. With the direct delivery by laser-induced photoporation, the NPs will be avoid being trapped in the endosome. The plasmonic nanomaterials, such as AuNPs, could be delivered into the cytoplasm for surface-enhanced Raman spectroscopy (SERS) to detect the intracellular PH, generation of reactive oxygen species, and gases. With an optimized delivery range, it will be very interesting to deliver the newly developed intracellular laser particles for intracellular tagging and tracking. [177]

Conclusion

Multiple strategies to deliver extrinsic probes into living cells are described in this review. Both biomedical agents and physical forces induced intracellular delivery strategies are presented in this review, including the delivery mechanisms, applications of labeling and advantages as well as disadvantages. Biomedical strategies provide the opportunity to deliver cell-impermeable probes by endocytosis or membrane poreration, which are easy-to-access and affordable for general recipients. Compared with biomedical methods, physical methods are at present the more versatile, offering direct intracellular delivery without endocytic uptake. Particularly, nanoparticle sensitized laser-induced photoporation and microfluidic cell squeezing seem to be the most promising as they combine fast treatment with ease of use, high delivery efficiency and cell viability. A general downside of physical membrane permeabilization methods is that they mostly rely on passive diffusion from the cell medium into the cytoplasm. Not only does this require a fairly high concentration of probes to be present in the cell medium, it greatly restricts the delivery efficiency of larger probes which diffuse more slowly. Therefore, one could compare those strategies and choose the most suitable method for intracellular delivery of extrinsic probes, depending on the specific requirement. More advanced intracellular delivery techniques are developed in recent years, like BLAST, which offers active transport of even very large cargo's into cells by combining photonics with microfluidics and nanofabrication. It is a striking example that the integration of several technologies may offer a valuable route for further development in the future.

Acknowledgment

K.B. acknowledges financial support from the European Research Council (ERC) under the European Union's Horizon 2020 research and innovation program (grant agreement No 648124) and from the Ghent University Special Research Fund (01B04912) with gratitude. J.L.

gratefully acknowledges the financial support from the China Scholarship Council (CSC) (201506750012) and the Ghent University Special Research Fund (01SC1416). J.F. gratefully acknowledges the financial support from FWO (1210120N). RX gratefully acknowledges the financial support from the Research Foundation Flanders (FWO, 1500418N and 12Q8718N).

References

1. Zhu, H.; Fan, J.; Du, J.; Peng, X., *Accounts of chemical research* **2016,** *49* (10), 2115-2126.
2. Derfus, A. M.; Chan, W. C.; Bhatia, S. N., *Advanced Materials* **2004,** *16* (12), 961-966.
3. Liu, J.-H.; Cao, L.; LeCroy, G. E.; Wang, P.; Meziani, M. J.; Dong, Y.; Liu, Y.; Luo, P. G.; Sun, Y.-P., *ACS applied materials & interfaces* **2015,** *7* (34), 19439-19445.
4. Zhang, X.; Zhang, X.; Yang, B.; Hui, J.; Liu, M.; Chi, Z.; Liu, S.; Xu, J.; Wei, Y., *Journal of Materials Chemistry C* **2014,** *2* (5), 816-820.
5. Ahrens, E. T.; Bulte, J. W. M., *Nature Reviews Immunology* **2013,** *13* (10), 755-763. DOI 10.1038/nri3531.
6. Neri, M.; Maderna, C.; Cavazzin, C.; Deidda-Vigoriti, V.; Politi, L. S.; Scotti, G.; Marzola, P.; Sbarbati, A.; Vescovi, A. L.; Gritti, A., *STEM CELLS* **2008,** *26* (2), 505-516. DOI 10.1634/stemcells.2007-0251.
7. Ahrens, E. T.; Zhong, J., *NMR in Biomedicine* **2013,** *26* (7), 860-871. DOI 10.1002/nbm.2948.
8. Estelrich, J.; Sánchez-Martín, M. J.; Busquets, M. A., *International journal of nanomedicine* **2015,** *10*, 1727.
9. Burtea, C.; Laurent, S.; Vander Elst, L.; Muller, R. N., Contrast agents: magnetic resonance. In *Molecular imaging I*, Springer: 2008; pp 135-165.
10. Ni, D.; Bu, W.; Ehlerding, E. B.; Cai, W.; Shi, J., *Chemical Society Reviews* **2017,** *46* (23), 7438-7468.
11. Derfus, A. M.; Chen, A. A.; Min, D.-H.; Ruoslahti, E.; Bhatia, S. N., *Bioconjugate chemistry* **2007,** *18* (5), 1391-1396.
12. Berguig, G. Y.; Convertine, A. J.; Shi, J.; Palanca-Wessels, M. C.; Duvall, C. L.; Pun, S. H.; Press, O. W.; Stayton, P. S., *Molecular Pharmaceutics* **2012,** *9* (12), 3506-3514. DOI 10.1021/mp300338s.
13. Mindell, J. A., *Annual review of physiology* **2012,** *74*, 69-86.
14. Martens, T. F.; Remaut, K.; Demeester, J.; De Smedt, S. C.; Braeckmans, K., *Nano Today* **2014,** *9* (3), 344-364.
15. Shete, H. K.; Prabhu, R. H.; Patravale, V. B., *Journal of nanoscience and nanotechnology* **2014,** *14* (1), 460-474.
16. Ray, M.; Lee, Y.-W.; Scaletti, F.; Yu, R.; Rotello, V. M., *Nanomedicine* **2017,** *12* (8), 941-952.
17. Qin, X.; Yu, C.; Wei, J.; Li, L.; Zhang, C.; Wu, Q.; Liu, J.; Yao, S. Q.; Huang, W., *Advanced Materials* **2019,** *31* (46), 1902791.
18. Al-Jamal, W. T.; Al-Jamal, K. T.; Bomans, P. H.; Frederik, P. M.; Kostarelos, K., *Small* **2008,** *4* (9), 1406-1415.
19. Feng, X.; Tang, Y.; Duan, X.; Liu, L.; Wang, S., *Journal of Materials Chemistry* **2010,** *20* (7), 1312-1316.
20. Wang, W.; Li, Y.; Cheng, L.; Cao, Z.; Liu, W., *Journal of Materials Chemistry B* **2013,** *2* (1), 46-48.
21. Petryayeva, E.; Algar, W. R.; Medintz, I. L., *Applied spectroscopy* **2013,** *67* (3), 215-252.
22. Medintz, I. L.; Uyeda, H. T.; Goldman, E. R.; Mattoussi, H., *Nature materials* **2005,** *4* (6), 435-446.
23. Guo, H.; Qian, H.; Sun, S.; Sun, D.; Yin, H.; Cai, X.; Liu, Z.; Wu, J.; Jiang, T.; Liu, X., *Chemistry Central Journal* **2011,** *5* (1), 1.
24. Zhang, L.; Xia, J.; Zhao, Q.; Liu, L.; Zhang, Z., *small* **2010,** *6* (4), 537-544.
25. Zhou, C.; Wu, H.; Wang, M.; Huang, C.; Yang, D.; Jia, N., *Materials Science and Engineering: C* **2017,** *78*, 817-825.
26. Zhang, X.; Zhang, X.; Wang, S.; Liu, M.; Zhang, Y.; Tao, L.; Wei, Y., *ACS applied materials & interfaces* **2013,** *5* (6), 1943-1947.
27. Bayles, A. R.; Chahal, H. S.; Chahal, D. S.; Goldbeck, C. P.; Cohen, B. E.; Helms, B. A., *Nano letters* **2010,** *10* (10), 4086-4092.
28. Sivaram, A. J.; Rajitha, P.; Maya, S.; Jayakumar, R.; Sabitha, M., *Wiley Interdisciplinary Reviews: Nanomedicine and Nanobiotechnology* **2015,** *7* (4), 509-533.

29. Merckx, P.; De Backer, L.; Van Hoecke, L.; Guagliardo, R.; Echaide, M.; Baatsen, P.; Olmeda, B.; Saelens, X.; Pérez-Gil, J.; De Smedt, S. C., *Acta biomaterialia* **2018,** *78*, 236-246.
30. Toita, S.; Hasegawa, U.; Koga, H.; Sekiya, I.; Muneta, T.; Akiyoshi, K., *Journal of nanoscience and nanotechnology* **2008,** *8* (5), 2279-2285.
31. Chiang, W.-H.; Ho, V. T.; Chen, H.-H.; Huang, W.-C.; Huang, Y.-F.; Lin, S.-C.; Chern, C.-S.; Chiu, H.-C., *Langmuir* **2013,** *29* (21), 6434-6443.
32. Abraham, A.; Natraj, U.; Karande, A. A.; Gulati, A.; Murthy, M. R.; Murugesan, S.; Mukunda, P.; Savithri, H. S., *Scientific reports* **2016,** *6*, 21803.
33. Kaczmarczyk, S. J.; Sitaraman, K.; Young, H. A.; Hughes, S. H.; Chatterjee, D. K., *Proceedings of the National Academy of Sciences* **2011,** *108* (41), 16998-17003.
34. Vercauteren, D.; Rejman, J.; Martens, T. F.; Demeester, J.; De Smedt, S. C.; Braeckmans, K., *Journal of controlled release* **2012,** *161* (2), 566-581.
35. Soenen, S. J.; Montenegro, J.-M.; Abdelmonem, A. M.; Manshian, B. B.; Doak, S. H.; Parak, W. J.; De Smedt, S. C.; Braeckmans, K., *Acta biomaterialia* **2014,** *10* (2), 732-741.
36. Vermeulen, L. M.; Brans, T.; De Smedt, S. C.; Remaut, K.; Braeckmans, K., *Nano Today* **2018,** *21*, 74-90.
37. Frankel, A. D.; Pabo, C. O., *Cell* **1988,** *55* (6), 1189-1193.
38. Green, M.; Loewenstein, P. M., *Cell* **1988,** *55* (6), 1179-1188.
39. Bechara, C.; Sagan, S., *FEBS letters* **2013,** *587* (12), 1693-1702.
40. Koren, E.; Torchilin, V. P., *Trends in molecular medicine* **2012,** *18* (7), 385-393.
41. Langel, Ü., Classes and Applications of Cell-Penetrating Peptides. In *CPP, Cell-Penetrating Peptides*, Springer: 2019; pp 29-82.
42. Torchilin, V. P., *Peptide Science* **2008,** *90* (5), 604-610.
43. Lindberg, S.; Copolovici, D. M.; Langel, Ü., *Therapeutic delivery* **2011,** *2* (1), 71-82.
44. Copolovici, D. M.; Langel, K.; Eriste, E.; Langel, U., *ACS nano* **2014,** *8* (3), 1972-1994.
45. Duchardt, F.; Fotin-Mleczek, M.; Schwarz, H.; Fischer, R.; Brock, R., *Traffic* **2007,** *8* (7), 848-866.
46. Herce, H. D.; Garcia, A. E., *Proceedings of the National Academy of Sciences* **2007,** *104* (52), 20805-20810.
47. Herce, H.; Garcia, A.; Litt, J.; Kane, R.; Martin, P.; Enrique, N.; Rebolledo, A.; Milesi, V., *Biophysical journal* **2009,** *97* (7), 1917-1925.
48. Binder, H.; Lindblom, G., *Biophysical journal* **2003,** *85* (2), 982-995.
49. Su, Y.; Mani, R.; Hong, M., *Journal of the American Chemical Society* **2008,** *130* (27), 8856-8864.
50. Palm-Apergi, C.; Lorents, A.; Padari, K.; Pooga, M.; Hallbrink, M., *The FASEB Journal* **2009,** *23* (1), 214-223.
51. Polyakov, V.; Sharma, V.; Dahlheimer, J. L.; Pica, C. M.; Luker, G. D.; Piwnica-Worms, D., *Bioconjugate chemistry* **2000,** *11* (6), 762-771.
52. Zhu, Z.; Tian, D.; Gao, P.; Wang, K.; Li, Y.; Shu, X.; Zhu, J.; Zhao, Q., *Journal of the American Chemical Society* **2018,** *140* (50), 17484-17491.
53. Ji, X.; Zhang, R.; Wang, Z.; Niu, S.; Ding, C., *ACS Applied Bio Materials* **2018,** *2* (1), 370-377.
54. Ruan, G.; Agrawal, A.; Marcus, A. I.; Nie, S., *Journal of the American Chemical Society* **2007,** *129* (47), 14759-14766.
55. Lei, Y.; Tang, H.; Yao, L.; Yu, R.; Feng, M.; Zou, B., *Bioconjugate chemistry* **2007,** *19* (2), 421-427.
56. Yong, X.; Yang, X.; Emory, S. R.; Wang, J.; Dai, J.; Yu, X.; Mei, L.; Xie, J.; Ruan, G., *Biomaterials science* **2018,** *6* (11), 3085-3095.
57. Herce, H. D.; Schumacher, D.; Schneider, A. F.; Ludwig, A. K.; Mann, F. A.; Fillies, M.; Kasper, M.-A.; Reinke, S.; Krause, E.; Leonhardt, H., *Nature chemistry* **2017,** *9* (8), 762.
58. Olson, E. S.; Jiang, T.; Aguilera, T. A.; Nguyen, Q. T.; Ellies, L. G.; Scadeng, M.; Tsien, R. Y., *Proceedings of the National Academy of Sciences* **2010,** *107* (9), 4311-4316.

59. Langel, Ü., Toxicity and Immune Response. In *CPP, Cell-Penetrating Peptides*, Springer: 2019; pp 339-357.
60. Saar, K.; Lindgren, M.; Hansen, M.; Eiríksdóttir, E.; Jiang, Y.; Rosenthal-Aizman, K.; Sassian, M.; Langel, Ü., *Analytical biochemistry* **2005,** *345* (1), 55-65.
61. El-Andaloussi, S.; Järver, P.; Johansson, H. J.; Langel, Ü., *The Biochemical Journal* **2007,** *407* (Pt 2), 285.
62. Gilbert, R., *Cellular and Molecular Life Sciences CMLS* **2002,** *59* (5), 832-844.
63. Bhakdi, S.; Tranum-Jensen, J.; Sziegoleit, A., *Infection and immunity* **1985,** *47* (1), 52-60.
64. Hotze, E. M.; Tweten, R. K., *Biochimica Et Biophysica Acta (BBA)-Biomembranes* **2012,** *1818* (4), 1028-1038.
65. Hotze, E. M.; Wilson-Kubalek, E.; Farrand, A. J.; Bentsen, L.; Parker, M. W.; Johnson, A. E.; Tweten, R. K., *Journal of Biological Chemistry* **2012,** *287* (29), 24534-24543.
66. Palmer, M.; Harris, R.; Freytag, C.; Kehoe, M.; Tranum‐Jensen, J.; Bhakdi, S., *The EMBO journal* **1998,** *17* (6), 1598-1605.
67. Walev, I.; Bhakdi, S. C.; Hofmann, F.; Djonder, N.; Valeva, A.; Aktories, K.; Bhakdi, S., *Proceedings of the National Academy of Sciences* **2001,** *98* (6), 3185-3190.
68. Teng, K. W.; Ishitsuka, Y.; Ren, P.; Youn, Y.; Deng, X.; Ge, P.; Belmont, A. S.; Selvin, P. R., *eLife* **2016,** *5*, e20378.
69. Rajapakse, H. E.; Gahlaut, N.; Mohandessi, S.; Yu, D.; Turner, J. R.; Miller, L. W., *Proceedings of the National Academy of Sciences* **2010,** *107* (31), 13582-13587.
70. Santangelo, P. J.; Lifland, A. W.; Curt, P.; Sasaki, Y.; Bassell, G. J.; Lindquist, M. E.; Crowe Jr, J. E., *Nature methods* **2009,** *6* (5), 347.
71. Etxaniz, A.; González-Bullón, D.; Martín, C.; Ostolaza, H., *Toxins* **2018,** *10* (6), 234.
72. Andrews, N. W.; Almeida, P. E.; Corrotte, M., *Trends in cell biology* **2014,** *24* (12), 734-742.
73. McNeil, P. L.; Vogel, S. S.; Miyake, K.; Terasaki, M., *J Cell Sci* **2000,** *113* (11), 1891-1902.
74. Teng, K. W.; Ren, P.; Selvin, P. R., *Current protocols in protein science* **2018,** *93* (1), e60.
75. Dal Peraro, M.; Van Der Goot, F. G., *Nature reviews microbiology* **2016,** *14* (2), 77.
76. Neumann, E.; Schaefer‐Ridder, M.; Wang, Y.; Hofschneider, P., *The EMBO journal* **1982,** *1* (7), 841-845.
77. Shi, J.; Ma, Y.; Zhu, J.; Chen, Y.; Sun, Y.; Yao, Y.; Yang, Z.; Xie, J., *Molecules* **2018,** *23* (11), 3044.
78. Stewart, M. P.; Langer, R.; Jensen, K. F., *Chemical reviews* **2018,** *118* (16), 7409-7531.
79. Kotnik, T.; Kramar, P.; Pucihar, G.; Miklavcic, D.; Tarek, M., *IEEE Electrical Insulation Magazine* **2012,** *28* (5), 14-23.
80. Crawford, R.; Torella, J. P.; Aigrain, L.; Plochowietz, A.; Gryte, K.; Uphoff, S.; Kapanidis, A. N., *Biophysical journal* **2013,** *105* (11), 2439-2450.
81. Canatella, P.; Prausnitz, M., *Gene therapy* **2001,** *8* (19), 1464.
82. Xie, X.; Xu, A. M.; Leal-Ortiz, S.; Cao, Y.; Garner, C. C.; Melosh, N. A., *ACS nano* **2013,** *7* (5), 4351-4358.
83. Huang, J.-A.; Caprettini, V.; Zhao, Y.; Melle, G.; Maccaferri, N.; Deleye, L.; Zambrana-Puyalto, X.; Ardini, M.; Tantussi, F.; Dipalo, M., *Nano letters* **2019,** *19* (2), 722-731.
84. He, G.; Feng, J.; Zhang, A.; Zhou, L.; Wen, R.; Wu, J.; Yang, C.; Yang, J.; Li, C.; Chen, D., *Nano letters* **2019**.
85. Kang, W.; Yavari, F.; Minary-Jolandan, M.; Giraldo-Vela, J. P.; Safi, A.; McNaughton, R. L.; Parpoil, V.; Espinosa, H. D., *Nano letters* **2013,** *13* (6), 2448-2457.
86. Moon, S.; Li, W.; Xu, K., *bioRxiv* **2019**, 642868.
87. Xiong, R.; Samal, S. K.; Demeester, J.; Skirtach, A. G.; De Smedt, S. C.; Braeckmans, K., *Advances in Physics: X* **2016,** *1* (4), 596-620.
88. Tsukakoshi, M.; Kurata, S.; Nomiya, Y.; Ikawa, Y.; Kasuya, T., *Applied Physics B* **1984,** *35* (3), 135-140.
89. Kurata, S.-I.; Tsukakoshi, M.; Kasuya, T.; Ikawa, Y., *Experimental cell research* **1986,** *162* (2), 372-378.

90. Tao, W.; Wilkinson, J.; Stanbridge, E. J.; Berns, M. W., *Proceedings of the National Academy of Sciences* **1987,** *84* (12), 4180-4184.
91. Tirlapur, U. K.; König, K., *Nature* **2002,** *418* (6895), 290.
92. Clark, I.; Hanania, E. G.; Stevens, J.; Gallina, M.; Fieck, A.; Brandes, R.; Palsson, B. O.; Koller, M. R., *Journal of biomedical optics* **2006,** *11* (1), 014034.
93. Lei, M.; Xu, H.; Yang, H.; Yao, B., *Journal of neuroscience methods* **2008,** *174* (2), 215-218.
94. Uchugonova, A.; König, K.; Bueckle, R.; Isemann, A.; Tempea, G., *Optics Express* **2008,** *16* (13), 9357-9364.
95. Hosokawa, Y.; Ochi, H.; Iino, T.; Hiraoka, A.; Tanaka, M., *PLoS One* **2011,** *6* (11), e27677.
96. Dhakal, K.; Black, B.; Mohanty, S., *Scientific reports* **2014,** *4*, 6553.
97. Rendall, H. A.; Marchington, R. F.; Praveen, B. B.; Bergmann, G.; Arita, Y.; Heisterkamp, A.; Gunn-Moore, F. J.; Dholakia, K., *Lab on a Chip* **2012,** *12* (22), 4816-4820.
98. Lukianova-Hleb, E. Y.; Belyanin, A.; Kashinath, S.; Wu, X.; Lapotko, D. O., *Biomaterials* **2012,** *33* (6), 1821-1826.
99. Lapotko, D., *Cancers* **2011,** *3* (1), 802-840.
100. Lapotko, D., *Nanomedicine* **2009,** *4* (7), 813-845.
101. Lukianova-Hleb, E. Y.; Mutonga, M. B.; Lapotko, D. O., *Acs Nano* **2012,** *6* (12), 10973-10981.
102. Xiong, R.; Joris, F.; Liang, S.; De Rycke, R.; Lippens, S.; Demeester, J.; Skirtach, A.; Raemdonck, K.; Himmelreich, U.; De Smedt, S. C., *Nano Letters* **2016,** *16* (10), 5975-5986.
103. Xiong, R.; Drullion, C.; Verstraelen, P.; Demeester, J.; Skirtach, A. G.; Abbadie, C.; De Vos, W. H.; De Smedt, S. C.; Braeckmans, K., *Journal of Controlled Release* **2017,** *266*, 198-204.
104. Xiong, R.; Verstraelen, P.; Demeester, J.; Skirtach, A. G.; Timmermans, J.-P.; De Smedt, S. C.; De Vos, W. H.; Braeckmans, K., *Frontiers in cellular neuroscience* **2018,** *12*, 80.
105. Liu, J.; Xiong, R.; Brans, T.; Lippens, S.; Parthoens, E.; Zanacchi, F. C.; Magrassi, R.; Singh, S. K.; Kurungot, S.; Szunerits, S., *Light: Science & Applications* **2018,** *7* (1), 47.
106. Pan, Y.; Neuss, S.; Leifert, A.; Fischler, M.; Wen, F.; Simon, U.; Schmid, G.; Brandau, W.; Jahnen-Dechent, W., *Small* **2007,** *3* (11), 1941-1949.
107. Schaeublin, N. M.; Braydich-Stolle, L. K.; Schrand, A. M.; Miller, J. M.; Hutchison, J.; Schlager, J. J.; Hussain, S. M., *Nanoscale* **2011,** *3* (2), 410-420.
108. Lachaine, R. m.; Boulais, E. t.; Meunier, M., *Acs Photonics* **2014,** *1* (4), 331-336.
109. Boulais, E. t.; Lachaine, R. m.; Meunier, M., *Nano letters* **2012,** *12* (9), 4763-4769.
110. Wu, Y.-C.; Wu, T.-H.; Clemens, D. L.; Lee, B.-Y.; Wen, X.; Horwitz, M. A.; Teitell, M. A.; Chiou, P.-Y., *Nature methods* **2015,** *12* (5), 439.
111. Madrid, M.; Saklayen, N.; Shen, W.; Huber, M.; Vogel, N.; Mazur, E., *ACS Applied Bio Materials* **2018,** *1* (6), 1793-1799.
112. Lyu, Z.; Zhou, F.; Liu, Q.; Xue, H.; Yu, Q.; Chen, H., *Advanced Functional Materials* **2016,** *26* (32), 5787-5795.
113. Wang, L.; Wu, J.; Hu, Y.; Hu, C.; Pan, Y.; Yu, Q.; Chen, H., *Journal of Materials Chemistry B* **2018,** *6* (27), 4427-4436.
114. Saklayen, N.; Huber, M.; Madrid, M.; Nuzzo, V.; Vulis, D. I.; Shen, W.; Nelson, J.; McClelland, A. A.; Heisterkamp, A.; Mazur, E., *ACS nano* **2017,** *11* (4), 3671-3680.
115. Messina, G. C.; Dipalo, M.; La Rocca, R.; Zilio, P.; Caprettini, V.; Proietti Zaccaria, R.; Toma, A.; Tantussi, F.; Berdondini, L.; De Angelis, F., *Advanced Materials* **2015,** *27* (44), 7145-7149.
116. Barber, M. A., *The Journal of Infectious Diseases* **1911**, 348-360.
117. Mertz, J. E.; Gurdon, J. B., *Proceedings of the National Academy of Sciences* **1977,** *74* (4), 1502-1506.
118. Anderson, W. F.; Killos, L.; Sanders-Haigh, L.; Kretschmer, P. J.; Diacumakos, E. G., *Proceedings of the National Academy of Sciences* **1980,** *77* (9), 5399-5403.
119. Capecchi, M. R., *Cell* **1980,** *22* (2), 479-488.
120. Holt, B. D.; Shawky, J. H.; Dahl, K. N.; Davidson, L. A.; Islam, M. F., *Journal of Applied Toxicology* **2016,** *36* (4), 568-578.

121. Xu, J.; Teslaa, T.; Wu, T.-H.; Chiou, P.-Y.; Teitell, M. A.; Weiss, S., *Nano letters* **2012,** *12* (11), 5669.
122. Wu, T.-H.; Sagullo, E.; Case, D.; Zheng, X.; Li, Y.; Hong, J. S.; TeSlaa, T.; Patananan, A. N.; McCaffery, J. M.; Niazi, K., *Cell metabolism* **2016,** *23* (5), 921-929.
123. Hennig, S.; Van De Linde, S.; Lummer, M.; Simonis, M.; Huser, T.; Sauer, M., *Nano letters* **2015,** *15* (2), 1374-1381.
124. Simonis, M.; Hübner, W.; Wilking, A.; Huser, T.; Hennig, S., *Scientific reports* **2017,** *7*, 41277.
125. Yun, C.-K.; Hwang, J. W.; Kwak, T. J.; Chang, W.-J.; Ha, S.; Han, K.; Lee, S.; Choi, Y.-S., *Lab on a Chip* **2019,** *19* (4), 580-588.
126. Chen, X.; Zhu, G.; Yang, Y.; Wang, B.; Yan, L.; Zhang, K. Y.; Lo, K. K. W.; Zhang, W., *Advanced healthcare materials* **2013,** *2* (8), 1103-1107.
127. Wang, Y.; Yang, Y.; Yan, L.; Kwok, S. Y.; Li, W.; Wang, Z.; Zhu, X.; Zhu, G.; Zhang, W.; Chen, X., *Nature communications* **2014,** *5*, 4466.
128. Xu, A. M.; Wang, D. S.; Shieh, P.; Cao, Y.; Melosh, N. A., *ChemBioChem* **2017,** *18* (7), 623-628.
129. Xu, A. M.; Aalipour, A.; Leal-Ortiz, S.; Mekhdjian, A. H.; Xie, X.; Dunn, A. R.; Garner, C. C.; Melosh, N. A., *Nature communications* **2014,** *5*, 3613.
130. Chiappini, C.; Martinez, J. O.; De Rosa, E.; Almeida, C. S.; Tasciotti, E.; Stevens, M. M., *ACS nano* **2015,** *9* (5), 5500-5509.
131. Chiappini, C.; De Rosa, E.; Martinez, J.; Liu, X.; Steele, J.; Stevens, M.; Tasciotti, E., *Nature materials* **2015,** *14* (5), 532.
132. Xie, X.; Xu, A. M.; Angle, M. R.; Tayebi, N.; Verma, P.; Melosh, N. A., *Nano letters* **2013,** *13* (12), 6002-6008.
133. Mumm, F.; Beckwith, K. M.; Bonde, S.; Martinez, K. L.; Sikorski, P., *Small* **2013,** *9* (2), 263-272.
134. Hanson, L.; Lin, Z. C.; Xie, C.; Cui, Y.; Cui, B., *Nano Letters* **2012,** *12* (11), 5815-5820. DOI 10.1021/nl303163y.
135. Zhao, W.; Hanson, L.; Lou, H.-Y.; Akamatsu, M.; Chowdary, P. D.; Santoro, F.; Marks, J. R.; Grassart, A.; Drubin, D. G.; Cui, Y., *Nature nanotechnology* **2017,** *12* (8), 750.
136. Gopal, S.; Chiappini, C.; Penders, J.; Leonardo, V.; Seong, H.; Rothery, S.; Korchev, Y.; Shevchuk, A.; Stevens, M. M., *Advanced Materials* **2019,** *31* (12), 1806788.
137. Elnathan, R.; Kwiat, M.; Patolsky, F.; Voelcker, N. H., *Nano Today* **2014,** *9* (2), 172-196.
138. Chen, Y.; Aslanoglou, S.; Gervinskas, G.; Abdelmaksoud, H.; Voelcker, N. H.; Elnathan, R., *Small* **2019**, 1904819.
139. Matsumoto, D.; Sathuluri, R. R.; Kato, Y.; Silberberg, Y. R.; Kawamura, R.; Iwata, F.; Kobayashi, T.; Nakamura, C., *Scientific reports* **2015,** *5*, 15325.
140. Sackmann, E. K.; Fulton, A. L.; Beebe, D. J., *Nature* **2014,** *507* (7491), 181-189.
141. Nge, P. N.; Rogers, C. I.; Woolley, A. T., *Chemical reviews* **2013,** *113* (4), 2550-2583.
142. Sharei, A.; Zoldan, J.; Adamo, A.; Sim, W. Y.; Cho, N.; Jackson, E.; Mao, S.; Schneider, S.; Han, M.-J.; Lytton-Jean, A., *Proceedings of the National Academy of Sciences* **2013,** *110* (6), 2082-2087.
143. Lee, J.; Sharei, A.; Sim, W. Y.; Adamo, A.; Langer, R.; Jensen, K. F.; Bawendi, M. G., *Nano letters* **2012,** *12* (12), 6322-6327.
144. Kollmannsperger, A.; Sharei, A.; Raulf, A.; Heilemann, M.; Langer, R.; Jensen, K. F.; Wieneke, R.; Tampé, R., *Nature communications* **2016,** *7*.
145. Klein, A.; Hank, S.; Raulf, A.; Joest, E. F.; Tissen, F.; Heilemann, M.; Wieneke, R.; Tampé, R., *Chemical science* **2018,** *9* (40), 7835-7842.
146. Liu, A.; Islam, M.; Stone, N.; Varadarajan, V.; Jeong, J.; Bowie, S.; Qiu, P.; Waller, E. K.; Alexeev, A.; Sulchek, T., *Materials Today* **2018,** *21* (7), 703-712.
147. Modaresi, S.; Pacelli, S.; Subham, S.; Dathathreya, K.; Paul, A., *Advanced Therapeutics*.
148. Han, X.; Liu, Z.; chan Jo, M.; Zhang, K.; Li, Y.; Zeng, Z.; Li, N.; Zu, Y.; Qin, L., *Science advances* **2015,** *1* (7), e1500454.
149. Saung, M. T.; Sharei, A.; Adalsteinsson, V. A.; Cho, N.; Kamath, T.; Ruiz, C.; Kirkpatrick, J.; Patel, N.; Mino‐Kenudson, M.; Thayer, S. P., *Small* **2016,** *12* (42), 5873-5881.

150. Deng, Y.; Kizer, M.; Rada, M.; Sage, J.; Wang, X.; Cheon, D.-J.; Chung, A. J., *Nano letters* **2018,** *18* (4), 2705-2710.
151. Dixit, H.; Starr, R.; Dundon, M. L.; Yang, X.; Zhang, Y.; Nampe, D.; Ballas, C. B.; Tsutsui, H.; Forman, S. J.; Brown, C., *Nano Letters* **2019**.
152. Kizer, M. E.; Deng, Y.; Kang, G.; Mikael, P. E.; Wang, X.; Chung, A. J., *Lab on a Chip* **2019,** *19* (10), 1747-1754.
153. Wang, W.; Duan, W.; Ahmed, S.; Mallouk, T. E.; Sen, A., *Nano Today* **2013,** *8* (5), 531-554.
154. Campuzano, S.; De Ávila, B. E.-F.; Yáñez-Sedeño, P.; Pingarron, J.; Wang, J., *Chemical science* **2017,** *8* (10), 6750-6763.
155. Li, J.; de Avila, B. E.-F.; Gao, W.; Zhang, L.; Wang, J., *Science Robotics* **2017,** *2* (4).
156. Sánchez, S.; Soler, L.; Katuri, J., *Angewandte Chemie International Edition* **2015,** *54* (5), 1414-1444.
157. Xu, T.; Gao, W.; Xu, L. P.; Zhang, X.; Wang, S., *Advanced Materials* **2017,** *29* (9), 1603250.
158. Li, T.; Zhang, A.; Shao, G.; Wei, M.; Guo, B.; Zhang, G.; Li, L.; Wang, W., *Advanced Functional Materials* **2018,** *28* (25), 1706066.
159. Esteban-Fernández de Ávila, B.; Martín, A.; Soto, F.; Lopez-Ramirez, M. A.; Campuzano, S.; Vásquez-Machado, G. M.; Gao, W.; Zhang, L.; Wang, J., *ACS nano* **2015,** *9* (7), 6756-6764.
160. Qualliotine, J. R.; Bolat, G.; Beltrán-Gastélum, M.; de Ávila, B. E.-F.; Wang, J.; Califano, J. A., *Otolaryngology–Head and Neck Surgery* **2019**, 0194599819866407.
161. Hansen‐Bruhn, M.; de Ávila, B. E. F.; Beltrán‐Gastélum, M.; Zhao, J.; Ramírez‐Herrera, D. E.; Angsantikul, P.; Vesterager Gothelf, K.; Zhang, L.; Wang, J., *Angewandte Chemie International Edition* **2018,** *57* (10), 2657-2661.
162. Solovev, A. A.; Xi, W.; Gracias, D. H.; Harazim, S. M.; Deneke, C.; Sanchez, S.; Schmidt, O. G., *Acs Nano* **2012,** *6* (2), 1751-1756.
163. Wang, W.; Wu, Z.; Lin, X.; Si, T.; He, Q., *Journal of the American Chemical Society* **2019,** *141* (16), 6601-6608.
164. Nain, S.; Sharma, N., *Frontiers in Life Science* **2015,** *8* (1), 2-17.
165. Li, T.; Li, J.; Morozov, K. I.; Wu, Z.; Xu, T.; Rozen, I.; Leshansky, A. M.; Li, L.; Wang, J., *Nano letters* **2017,** *17* (8), 5092-5098.
166. Xu, T.; Xu, L.-P.; Zhang, X., *Applied Materials Today* **2017,** *9*, 493-503.
167. Xu, X.; Hou, S.; Wattanatorn, N.; Wang, F.; Yang, Q.; Zhao, C.; Yu, X.; Tseng, H.-R.; Jonas, S. J.; Weiss, P. S., *ACS nano* **2018,** *12* (5), 4503-4511.
168. García-López, V.; Chen, F.; Nilewski, L. G.; Duret, G.; Aliyan, A.; Kolomeisky, A. B.; Robinson, J. T.; Wang, G.; Pal, R.; Tour, J. M., *Nature* **2017,** *548* (7669), 567.
169. Schinkel, H.; Jacobs, P.; Schillberg, S.; Wehner, M., *Biotechnology and bioengineering* **2008,** *99* (1), 244-248.
170. Sengupta, A.; Kelly, S. C.; Dwivedi, N.; Thadhani, N.; Prausnitz, M. R., *ACS nano* **2014,** *8* (3), 2889-2899.
171. Raun, A.; Saklayen, N.; Zgrabik, C.; Shen, W.; Madrid, M.; Huber, M.; Hu, E.; Mazur, E., *Scientific reports* **2018,** *8* (1), 15595.
172. Xiong, R.; Verstraelen, P.; Demeester, J.; Skirtach, A.; Timmermans, J.-P.; De Smedt, S.; De Vos, W. H.; Braeckmans, K., *Frontiers in Cellular Neuroscience* **2018,** *12*, 80.
173. Klein, A.; Hank, S.; Raulf, A.; Joest, E.; Tissen, F.; Heilemann, M.; Wieneke, R.; Tampé, R., *Chemical science* **2018,** *9* (40), 7835-7842.
174. Li, Y.; Wu, M. X.; Zhao, D. Y.; Wei, Z. W.; Zhong, W. F.; Wang, X. X.; Liang, Z. C.; Li, Z. H., *Sci Rep-Uk* **2015,** *5*. DOI ARTN 17817

10.1038/srep17817.
175. Wu, Y.-C.; Wu, T.-H.; Clemens, D. L.; Lee, B.-Y.; Wen, X.; Horwitz, M. A.; Teitell, M. A.; Chiou, P.-Y., *Nature methods* **2015,** *12* (5), 439-444.
176. Rosazza, C.; Buntz, A.; Rieß, T.; Wöll, D.; Zumbusch, A.; Rols, M.-P., *Molecular therapy* **2013,** *21* (12), 2217-2226.

177. Martino, N.; Kwok, S. J.; Liapis, A. C.; Forward, S.; Jang, H.; Kim, H.-M.; Wu, S. J.; Wu, J.; Dannenberg, P. H.; Jang, S.-J., *Nature Photonics* **2019,** *13* (10), 720-727.

Brief summary

This review provides a new horizon for intracellular delivery of extrinsic probes (cell-impermeable), including both biomedical and physical strategies. Borrowed from gene delivery methods, different biomedical agents are used in this case for intracellular delivery of probes mostly through endocytosis. While different physical forces are applied for direct intracellular delivery by cell-membrane disruption, inducing much higher efficiency than biomedical methods.

Keyword

Intracellular labeling

J. Liu, J. C. Fraire, S. C. De Smedt, R. Xiong, K. Braeckmans*

Title

Intracellular labeling with extrinsic probes: delivery strategies and applications